The ketone body β-hydroxybutyrate rescues GABAergic defects in *C. elegans daf-18/PTEN* mutants

Sebastián Giunti[1,2], María Gabriela Blanco[1,2], María José De Rosa[1,2*] and Diego Rayes[1,2*]

1-Instituto de Investigaciones Bioquímicas de Bahía Blanca (INIBIBB) CCT UNS-CONICET, Bahía Blanca, Argentina

2-Departamento de Biología, Bioquímica y Farmacia, Universidad Nacional Del Sur (UNS), Bahía Blanca, Argentina

Correspondence to:

Maria José De Rosa (mjderosa@criba.edu.ar)

Diego Rayes (drayes@criba.edu.ar)

Abstract (175 words)

Increased Excitation/Inhibition (E/I) ratios in the brain are hallmarks of neurological disorders, such as Autism Spectrum Disorders (ASD). Mutations in PTEN, the main PI3K/Akt pathway negative regulator, are strongly associated with ASD. It is unclear how PTEN deficiencies lead to E/I disequilibrium. Using *C. elegans* neuromuscular system as a model for studying E/I balance, we find that *daf-18/PTEN* mutations affect GABAergic (but not cholinergic) neurodevelopment, leading to behavioral phenotypes typical of an increased E/I ratio. The specific defects in GABAergic development in *daf-18/PTEN* mutants are due to the reduced activity of DAF-16/FOXO3A. Ketogenic diets (KGDs) are effective approaches for disorders associated with E/I imbalances. However, their mechanisms of action are not understood. We show, in *daf-18/PTEN* mutants, that a diet enriched with the ketone body hydroxybutyrate during early development improves GABAergic neurodevelopment and rescued behavioral defects in a DAF-16/FOXO-dependent manner. Our study offers universal insights into the proven link between PTEN mutations and neurodevelopmental defects and provides new insights into the mechanisms underlying KGDs' positive effects on neuronal disorders characterized by E/I imbalances.

INTRODUCTION

A fine-tuned balance between excitatory and inhibitory (E/I) neurotransmission is crucial for optimal brain function (Tao, Li et al., 2014). A large body of evidence suggests that disruption of this balance is a key feature of several neuronal pathologies (Rubenstein & Merzenich, 2003). In particular, it has been shown that deficits in inhibitory (GABAergic) signaling are frequent in Autism Spectrum Disorders (ASD) and other neurodevelopmental disorders (Bozzi, Provenzano et al., 2018, Coghlan, Horder et al., 2012, Oblak, Gibbs et al., 2009). While the exact causes of ASD are unknown, it has been proposed that a combination of genetic and environmental risk factors is involved. Interestingly, GABAergic system deficiency has been reported in both ASD-associated genetic backgrounds and pharmacologically-induced murine models of ASD (Gogolla, Leblanc et al., 2009). The molecular and cellular mechanisms underlying these typical E/I imbalances in neurodevelopmental disorders are largely unclear.

PTEN (phosphatase and tensin homolog deleted on chromosome 10) is a classical tumor suppressor gene that antagonizes the phosphatidylinositol 3-phosphate kinase (PI3K)/protein kinase B (PKB/Akt) pathway. This highly conserved pathway is a master regulator of cell proliferation, differentiation, and cell death. *PTEN* encodes a lipid and protein phosphatase that hydrolyzes phosphatidylinositol (3,4,5)-trisphosphate (PIP_3) to phosphatidylinositol-4,5-bisphosphate (PIP_2), therefore inhibiting Akt activity (Maehama & Dixon, 1998). Due to its key role in the PI3K/Akt pathway, mutations in PTEN are typically associated with tumorigenesis (Li, Yen et al., 1997, Radu, Neubauer et al., 2003). Beyond this widely studied regulatory function in cell proliferation, in the last 20 years, several reports have highlighted the importance of PTEN and the PI3K/Akt pathway in neurodevelopment (Rademacher & Eickholt, 2019). For instance, PTEN deletions in cultured mouse neurons result in hypertrophy, ectopic axon formation, and excessive branching (van Diepen & Eickholt, 2008). Moreover, *PTEN* KO animals exhibit an imbalance between E/I (Lee, Lee et al., 2017) and develop behavioral abnormalities such as communication and cognitive deficits and repetitive behaviors (Kwon, Luikart et al., 2006, Smith,

White et al., 2016). Mutations in *PTEN* were frequently found in human patients presenting ASD (Butler, Dasouki et al., 2005). The Simons Foundation Autism Research Initiative (SFARI) has assigned *PTEN* a gene scoring of 1 (High confidence), which reflects the strong association between this gene and ASD. As with other genes related to neurodevelopmental disorders, the events underlying the E/I imbalance and the resulting neurodevelopmental deficits in *PTEN* mutants remain poorly understood.

Ketogenic diets (KGDs), which are very high in fat and low in carbohydrates, are thought to simulate the metabolic effects of fasting by forcing the use of fat as a fuel source via fatty acids beta-oxidation into the ketone bodies (KBs): acetoacetate, β-hydroxybutyrate (βHB), and acetone. These diets have been used for decades for the treatment of epilepsies (D'Andrea Meira, Romao et al., 2019). Even today, they are still useful in reducing the frequency of seizures in refractory epilepsies (Lambrechts, de Kinderen et al., 2017, Neal, Chaffe et al., 2008). More recently, KGDs have been shown to be effective in alleviating autistic symptoms both in humans (Li, Liang et al., 2021) and in rodent models of ASD (Castro, Baronio et al., 2017, Verpeut, DiCicco-Bloom et al., 2016). Both epilepsy and ASD share a common feature: the breakdown of the equilibrium between E/I (Bozzi et al., 2018). It is completely unknown how the KGDs exert these beneficial effects.

The mammalian brain contains billions of neurons each with the ability to make thousands of synaptic connections. This complexity makes it exceedingly difficult to study molecular and cellular underpinnings of neurodevelopment. The simplicity of invertebrate nervous systems has provided fundamental insights into universal neural processes ranging from neural development, axon guidance and neurotransmission, to circuit function and behavior. For instance, the *C. elegans* neuromuscular system, where both excitatory (cholinergic) and inhibitory (GABAergic) motor neurons regulate muscle activity, provides an attractive and complementary model for studying E/I balance (Huang, Pirri et al., 2019, Safdie, Liewald et al., 2016, Stawicki, Zhou et al., 2011, Vashlishan, Madison et al., 2008, Zhou & Bessereau, 2019).

Importantly, most of the main components of the PI3K/Akt pathway are conserved in *C. elegans* (Ogg & Ruvkun, 1998, Paradis & Ruvkun, 1998).

In this work, we examined the effect of the PTEN ortholog, DAF-18, on E/I balance in the *C. elegans* neuromuscular system. We find that *daf-18* mutants exhibit phenotypes typical of animals where the E/I ratio is increased. This imbalance is due to selective impairments in the neurodevelopment of GABAergic inhibitory motor neurons. Surprisingly, cholinergic excitatory motor neurons are not affected in these mutants. We also find that these neurodevelopmental deficits are due to reduced activity of the transcription factor DAF-16/FOXO. Interestingly, we demonstrate that exposure of these mutant animals to the KB βHB early during development increases DAF-16 activity, ameliorates morphological defects in the GABAergic neurons, and improves animal behavioral phenotypes. This work provides a behavioral simple system to study the role of the universally conserved PI3K/Akt/FOXO pathway in neurodevelopment, and could constitute a key step towards understanding the mechanisms of action of KBs and their potential therapeutic use in disorders associated with E/I imbalance.

RESULTS

Disturbances in the *C. elegans* E/I ratio can be detected by analyzing the sensitivity to the paralyzing effects of drugs that exacerbate cholinergic transmission (Huang et al., 2019, Vashlishan et al., 2008). To determine the role of *daf-18* (the *PTEN* orthologue in worms) in the E/I balance, we analyzed the sensitivity of *daf-18* deficient animals to the acetylcholinesterase inhibitor aldicarb and to the cholinergic agonist levamisole. We found that these mutants are hypersensitive to the paralyzing effects of both drugs (Fig. 1*A* and *B*, Fig.S1*B* and *C*). Increased sensitivity to these cholinergic drugs suggests an increased E/I ratio compared to control worms (Huang et al., 2019, Maglioni, Schiavi et al., 2022).

Reduced activity of DAF-18 has been largely shown to exacerbate the PI3K pathway, precluding the activation of DAF-16, the *C. elegans* ortholog of the FOXO transcription factors

family (Ogg & Ruvkun, 1998) (Fig. S2). We analyzed aldicarb and levamisole sensitivity of mutants in this transcription factor (Fig. 1*A* and *B*). Similar to *daf-18* mutants, we found that *daf-16* null mutants are hypersensitive to the paralyzing effects of aldicarb and levamisole (Fig. 1*A* and *B*). Furthermore, we did not observe significant differences in aldicarb and levamisole sensitivity between *daf-18; daf-16* double null mutants and the respective single mutants, suggesting that both genes affect neuromuscular signaling by acting in the same pathway (Fig. 1*A* and *B*).

Hypersensitivity to cholinergic drugs has long been observed in worms where there is a deficiency in GABAergic signaling (Huang et al., 2019, Vashlishan et al., 2008) (Fig. 1*A* and *B*). In mutants with severe deficits in GABA transmission, prodding induces a bilateral contraction of the body wall muscles that shortens the body (shrinker phenotype) (McIntire, Jorgensen et al., 1993). When *daf-18* mutants are touched, there is a slight but significant shortening in body length (Fig. 1*C*). As expected, this shortening is not as noticeable as in animals with a complete deficit in GABAergic signaling, such as mutants in *unc-25* (the *C. elegans* orthologue for glutamic acid decarboxylase) (Fig. 1*C*). Similar to *daf-18* mutants, *daf-16* animals also exhibit a mild decrease in body length after prodding. Consistent with our aldicarb and levamisole results, there are no significant differences in body shortening between *daf-18; daf-16* double mutants and the corresponding single mutants (Fig. 1*C*), further supporting the notion that both genes act in the same pathway to impact neuromuscular signaling.

We also analyzed other behaviors that require a concerted activity of GABAergic and cholinergic systems, such as the omega turns during the escape response (Donnelly, Clark et al., 2013). In *C. elegans* the escape response can be induced by a gentle touch on the head and involves a backward movement that is usually followed by a sharp omega turn and a 180° change in its direction of locomotion (Donnelly et al., 2013) (Movie 1). It is a complex behavior that requires a high degree of coordination between sensory perception, and the activation and inhibition of different motor programs (Pirri & Alkema, 2012). The execution of the omega turn

involves a hypercontraction of the ventral muscles and relaxation of the dorsal muscles (see Fig. 1*D*), allowing the animal to make a sharp turn, where the animal's head slides on the ventral side of the body (closed omega turn), and resume locomotion in the opposite direction. In response to anterior touch the vast majority of the wild-type worms make a closed omega turn. Ventral muscle contraction is triggered by cholinergic motor neurons (VA and VB neurons) that synapse onto ventral muscles, while dorsal muscle relaxation is induced by GABAergic motor neurons (DD neurons) that synapse onto dorsal muscles (Donnelly et al., 2013, Pirri & Alkema, 2012). Ablation of DD GABAergic neurons leads to a dramatic decrease in the frequency of closed omega turns (Donnelly et al., 2013). In agreement with previous reports, we found that 93% of wild-type animals exert a complete omega turn within the escape response (Fig. 1*D*). We observed that, similar to wild-type animals, *daf-18* mutants move backward upon gentle anterior touch with an eyelash (Movie 2). However, only 54% of *daf-18* mutant animals exhibit the typical head to tail contact during the omega turn (Fig. 1*D*). Similar to *daf-18* mutants, *daf-16* mutants exhibited a decrease in the proportion of closed omega turns (Fig. 1*D*). No additive effects were observed in the *daf-18; daf-16* double mutant, suggesting that the increased inactivation of *daf-16* is primarily responsible for the defects observed in the escape response of *daf-18* mutants.

It has been reported both in neuronal cultures and in animal models that mutations in *PTEN* lead to morphological alterations in neuronal processes (Christensen, de la Torre-Ubieta et al., 2011, Kennedy, Pham et al., 2013, van Diepen & Eickholt, 2008). Since our previous results suggest perturbations of neuromuscular transmission, we explored the morphology of *C. elegans* motor neurons. *C. elegans* body wall muscles are innervated by excitatory (cholinergic) and inhibitory (GABAergic) motor neurons (McIntire et al., 1993, White, Southgate et al., 1986). The cell bodies of both cholinergic (A and B-type) and GABAergic (D-type) motor neurons are located in the ventral nerve cord (VNC), and a subset extends single process commissures to the dorsal nerve cord (DNC) (Altun & Hall, 2011) (Fig. 2*A* and *D*). These commissures allowed

us to study defects in the development or maintenance of GABAergic and cholinergic neuronal processes (Caceres Ide, Valmas et al., 2012, Oliver, Norman et al., 2019). We analyzed the morphology of GABAergic motor neurons in L4 animals expressing mCherry under the control of the *unc-47* (worm orthologue for the vesicular GABA transporter SLC32A1) promoter (Byrne, McWhirter et al., 2016). We found that *daf-18* mutants exhibit a significantly higher frequency of commissure defects, including guidance defects, ectopic branching, and commissures that fail to reach the dorsal cord (Fig. 2*B*). GABAergic neuron anomalies were also evident at the first larval stage (L1), suggesting that reduced DAF-18/PTEN activity affects the neurodevelopment of the GABAergic system (Fig. S3). Since the transcription factor DAF-16/FOXO is one of the main targets of DAF-18/PTEN signaling, we analyzed the morphology of GABAergic D-type neurons in *daf-16* null mutants. These animals also exhibit an increased number of defects in commissures compared to the wild-type (Fig. 2*C*). Interestingly, the frequency of defects on *daf-18; daf-16* double mutants are similar to those observed in the single mutants, suggesting, again, that both genes act in the same pathway.

In contrast to our findings in GABAergic D-type neurons, we observed no obvious differences in the frequency of commissure defects when we compared the morphology of cholinergic motor neurons in control and *daf-18* animals (Fig. 2*D* and *E*). We, therefore, hypothesize that the morphological defects in inhibitory GABAergic neurons underlies the E/I imbalance in *daf-18/PTEN* mutants.

Given that *daf-18* is ubiquitously expressed in all tissues (Ogg & Ruvkun, 1998), we asked whether DAF-18 acts autonomously in GABAergic neurons to ensure proper development. We found that specific *daf-18* expression in GABAergic neurons partially rescued the behavioral phenotype of *daf-18* null mutants (Fig. 3*A*). In addition, the morphological defects in GABAergic commissures were significantly reduced (Fig. 3*B*). This suggests that DAF-18 acts autonomously in GABAergic motor neurons to regulate their development.

Taken together, we have shown that mutations in *daf-18* and *daf-16* lead to morphological defects in GABAergic neurons, without visibly affecting cholinergic motor neurons. Our pharmacological and behavioral experiments suggest that hyperactivation of the PI3K pathway, and the resulting DAF-16 inhibition, generates an increased E/I ratio in the *C. elegans* neuromuscular system.

Mutations in PTEN are linked with Autism Spectrum Disorders (ASD) (Rademacher & Eickholt, 2019). Ketogenic diets, which force the endogenous production of ketone bodies (KBs), have proved to be effective for the treatment of neurological disorders associated with E/I imbalances, such as epilepsy and, more recently, ASD (Lambrechts et al., 2017, Li et al., 2021, Neal et al., 2008). Since the observed defects in the GABAergic signal of *daf-18* mutants are likely to be a consequence of reduced DAF-16 activity, we asked whether it is possible to improve the observed phenotypes by modulating the activity of DAF-16. It has been shown that the KB βHB induces DAF-16 activity (Edwards, Canfield et al., 2014). To confirm these previous results, we evaluated the expression of *sod-3*, which codes for a superoxide dismutase and is a DAF-16 transcriptional target gene. We used a strain expressing a GFP transcriptional reporter for *sod-3* and determined fluorescence intensity upon dietary supplementation of βHB. Consistent with previous findings, we found that βHB (20 mM) induces *sod-3* expression in *daf-18* mutants, but we did not detect increased *sod-3* expression in *daf-16* deficient animals (Fig. S*4*).

Next, we evaluated behavioral phenotypes and GABAergic neuronal morphology of animals that were raised on an *E. coli* diet supplemented with 20 mM βHB throughout development. We found that βHB supplementation significantly reduced the hypersensitivity of *daf-18* mutants to the cholinergic drugs aldicarb and levamisole (Fig. 4*A* and *B*). Moreover, βHB supplementation rescued the post-prodding shortening in *daf-18* mutants (Fig. S5). Accordingly, we found that *daf-18* mutants showed a significant increase in the proportion of closed omega turns during their escape response compared to the naïve condition (Fig. 4*C*). In contrast, βHB exposure

does not change the number of closed omega turns in *daf-16* null mutants or the double null mutant *daf-18; daf-16* (Fig. 4*C*).

We also evaluated the morphology of GABAergic motor neurons in *daf-18* mutants exposed to βHB throughout development (from embryogenesis to L4). We found that βHB supplementation reduced the frequency of defects in GABAergic processes (Fig. 4*D*). Consistent with our observations on the closed omega turns frequency, βHB exposure did not significantly reduce the defects on GABAergic neurons of either *daf-16* null mutants or *daf-18; daf-16* double mutants. Taken together, these results demonstrate that dietary βHB ameliorates the defects associated with deficient GABAergic signaling in *daf-18* mutants.

It is noteworthy that we did not observe any improvement in either neuronal outgrowth defects in the AIY interneuron or in the migration of the HSN motor neurons (Fig. S6) in *daf-18* mutants, even though these defects were shown to depend on the reduction of DAF-16 activity (Christensen et al., 2011, Kennedy et al., 2013). Unlike the development of D-type GABAergic neurons that mainly occurs at L1 larval stages (White, Albertson et al., 1978), AIY neurite and HSN soma migration take place during embryogenesis (Christensen et al., 2011, Hedgecock, Culotti et al., 1987). It is therefore possible, that βHB may not go through the impermeable chitin egg shell of the embryo, as have been reported with other drugs (Sato, Sato et al., 2006).

In the above experiments, βHB was supplemented throughout development: from embryonic stages to the L4 larval stage. We next asked whether there is a critical period during development where the action of βHB is required. We exposed *daf-18* mutant animals to βHB supplemented diets at different periods of development (Fig. 5*A*). Interestingly, we found that exposure to βHB during early development (L1) was sufficient to increase the proportion of *daf-18* mutant animals executing a closed omega turn during the escape response. However, when the animals were exposed to βHB at later juvenile stages (L2-L3 or L3-L4), its ability to enhance the escape response of *daf-18* mutants declined (Fig. 5*B*). Moreover, exposing animals to βHB solely at the L1 stage was enough to reduce morphological defects in the GABAergic motor

neurons of this mutants (Fig. 5*C*). Thus, it is likely that βHB acts at very early stages of development to mitigate neurological defects in *daf-18* mutants.

Taken together, we show that deficiency of the *PTEN* ortholog in worms, *daf-18*, impairs the neurodevelopment of GABAergic neurons without affecting cholinergic neurons, leading to an E/I imbalance in the animal's neuromuscular system. Moreover, our results suggest that this imbalance is due to decreased activity of the transcription factor DAF-16/FOXO in the developing GABAergic neurons. In turn, exposure to βHB during the early neurodevelopmental stages compensates the low activity of DAF-16/FOXO in *daf-18/PTEN* mutants, therefore ameliorating the GABAergic deficit and the E/I imbalance (Fig. 6).

DISCUSSION

In this work, we demonstrate that loss-of-function mutations in *daf-18*, the *C. elegans* orthologue for *PTEN*, produces an E/I imbalance in the neuromuscular system. The imbalance arises due to specific defects on GABAergic motor neuron development. These GABA-specific deficiencies manifest as hypersensitivity to cholinergic drugs, mild body shortening after touch stimulus, and deficits in the execution of behaviors that require significant inhibitory signaling to the muscles, such as the omega turn during the escape response. We determined that these impairments in GABAergic development are due to reduced activity of the FOXO orthologue DAF-16 in *daf-18* mutants. Importantly, we also found that exposure to the ketone body βHB during early developmental stages ameliorates the deleterious effects of *daf-18* mutations, and that this protective effect of βHB depends on its capacity to induce DAF-16 activity.

Mutations in *daf-18/PTEN* have been linked to neurodevelopmental defects from worms to mammals. In humans, mutations in this gene are strongly associated with disorders such as ASD (Rademacher & Eickholt, 2019). An imbalance between synaptic excitation and inhibition is considered a key pathological mechanism linked to ASD-related behaviors (Bozzi et al., 2018, Rubenstein & Merzenich, 2003). Moreover, decreased activity of PTEN has been shown to

250 produce E/I disequilibrium and the development of seizures in mice (van Diepen & Eickholt,
251 2008). The mechanisms underlying this imbalance between excitatory and inhibitory signals are
252 not clear. Our results demonstrate that reduced DAF-18 activity generates guidance defects,
253 abnormal branching, and incomplete commissural outgrowth of inhibitory GABAergic neurons,
254 without affecting the morphology of excitatory cholinergic neurons. This specific impairment in
255 GABAergic neurodevelopment underlies the phenotypes observed in *daf-18/PTEN* mutants.
256 *daf-18* deficient mutants have a shorter lifespan (Mihaylova, Borland et al., 1999). One
257 possibility is that the defects observed in GABAergic processes are due to neurodegeneration
258 associated with premature aging rather than developmental flaws. However, this idea is unlikely
259 given that the GABAergic neuronal defects are already manifest at the L1 stage. In *C. elegans*,
260 the GABAergic motor neurons rearrange during larval development (Baran, Castelblanco et al.,
261 2010). Animals are born with six DD motor neurons that extend commissures to the dorsal side,
262 but initially only form synapses on the ventral muscles of the animal. Later on, 13 VD neurons
263 are born during the L1 stage and form synapses in ventral muscle cells. The preexisting ventral
264 synapses made by DD neurons are eliminated and new DD synapses form on the dorsal
265 muscles (White et al., 1978). This remodeling of DD neurons is complete by late L2 (Petersen,
266 Watson et al., 2011). Since the commissures are defective already at the early L1 stage (prior to
267 rewiring), we can infer that this specific impairment in the neurodevelopment of GABAergic
268 motor neurons is not a consequence of deficient GABAergic rearrangement during the early
269 larval stages.
270 Strikingly, cholinergic neurons have no noticeable morphological defects in *daf-18* mutants.
271 Loss-of-function mutants in the neuronal integrin *ina-1,* ortholog of human ITGA6, affect the
272 guidance of GABAergic commissures, without affecting cholinergic neurons (Oliver et al., 2019).
273 Similar to PTEN, mutations in neuronal integrins have been linked to neurodevelopmental
274 defects (Wu & Reddy, 2012). Interestingly, the PI3K/Akt/FOXO pathway and integrin signaling
275 are interrelated in mammals (Moreno-Layseca & Streuli, 2014). This observation opens the

possibility that one of the mechanisms by which *daf-18* mutants have defects in GABAergic neurodevelopment involves integrin expression and /or function.

In mammals, defects in *PTEN* mutants have been typically related to hyperactivation of the mTOR pathway (Cupolillo, Hoxha et al., 2016, Kwon et al., 2006). However, our results suggest that, in the *C. elegans* neuromuscular system, decreased activity of DAF-18 leads to an increase in the E/I ratio due to a downregulation of DAF-16/FOXO transcription factor activity. The FOXO family of transcription factors is conserved throughout the animal kingdom (Arden, 2008). There is increasing evidence demonstrating the key role of this transcription factors family in neurodevelopment (Santo & Paik, 2018). Downregulation of FOXO activity early in development reproduces neuropathological features found in ASD patients, i.e., increased brain size and cortical thickness (Khundrakpam, Lewis et al., 2017, Paik, Ding et al., 2009). The autonomic activity of the PI3K signaling coordinates axonal outgrowth in *C. elegans* AIY interneurons and rat cerebellar granule neurons (Christensen et al., 2011). On the other hand, DAF-18 and DAF-16 activity in *C. elegans* hypodermis modulates neuronal migration of the HSN neuron during development (Kennedy et al., 2013). Our rescue experiments strongly suggest that the PI3K/AKT-1/DAF-16 pathway modulates the development of GABAergic motor neurons by acting autonomously in these cells. Noteworthy, autonomic DAF-16 activity in GABAergic motor neurons is also key for axonal growth during regeneration (Byrne, Walradt et al., 2014). These results further emphasize the importance of DAF-16/FOXO in neuronal development and axonal growth.

In view of our findings and previous reports, a question arises as to which FOXO-dependent mechanisms might mediate neurodevelopmental defects. It has been shown that the autophagic flux is severely impaired in the neurogenesis of FOXO-deficient mice, leading to morphological defects (Schaffner, Minakaki et al., 2018). In *C. elegans*, reduced DAF-16 activity also negatively modulates autophagy (Palmisano & Melendez, 2019). Growing evidence supports a conserved link between aberrant autophagy signaling and neurodevelopmental defects (Collier,

302 Guissart et al., 2021, Stavoe, Hill et al., 2016). In this context, it would be interesting to study
303 whether early developmental FOXO activity modulates autophagic processes to ensure proper
304 neuronal development. Another potential mechanism may involve the p21-activating kinase
305 PAK1, a critical direct target gene of the DAF-16/FOXO transcription factors, that modulates
306 neurodevelopment (de la Torre-Ubieta & Bonni, 2011, Kennedy et al., 2013). Genetic ablation of
307 PAK1 in mice selectively suppresses GABAergic signaling (Xia, Zhou et al., 2018). Since our
308 rescue experiments suggest that DAF-16 acts in GABAergic cells, it is possible that PAK-1
309 plays an important role in GABAergic morphogenesis by acting autonomously in these motor
310 neurons. In contrast to this hypothesis, no expression of this kinase has been reported in
311 GABAergic motor neurons of L4 animals (https://cengen.shinyapps.io/CengenApp/). However,
312 we cannot totally rule this out, as there could be a transient expression of PAK-1 in GABAergic
313 neurons during the early larval stages. Further studies are needed to shed light on the
314 molecular mechanisms underlying the role of the PI3K/Akt/FOXO pathway in
315 neurodevelopment.
316 In many patients suffering from epilepsy, ketogenic diets can control seizures and reduce
317 behavioral problems (Lambrechts et al., 2017, Neal et al., 2008). Furthermore, they can reduce
318 behavioral abnormalities in patients suffering from ASD (Li et al., 2021). While the mechanisms
319 underlying the clinical effects of ketogenic diets remain unclear, it has been shown that these
320 diets correlate with increased GABA signaling (Calderon, Betancourt et al., 2017, Cantello,
321 Varrasi et al., 2007, Yudkoff, Daikhin et al., 2008). We demonstrate here that dietary
322 supplementation of the ketone body βHB ameliorates morphological defects in GABAergic
323 motor neurons of *daf-18* mutants, therefore alleviating the E/I imbalance on these animals.
324 Although ketone bodies were historically viewed as simple carriers of energy to peripheral
325 tissues during prolonged fasting or exercise, our findings confirm more recent reports showing
326 that βHB also possesses a variety of important signaling functions (Newman & Verdin, 2017).
327 We can hypothesize several distinct, non-mutually exclusive models by which βHB can induce

DAF-16/FOXO-dependent signaling. βHB directly inhibits mammalian histone deacetylases HDAC1 and HDAC2, increasing histone acetylation at the FOXO3a promoter and inducing the expression of this gene (Shimazu, Hirschey et al., 2013). HDAC1 and HDAC2 play an important role as redundant regulators of neuronal development (Park, Lee et al., 2022). Interestingly, in *C. elegans* βHB inhibits the class I HDACs to extend worm lifespan in a DAF-16-dependent manner (Edwards et al., 2014). Therefore, it is possible that βHB-mediated HDAC inhibition upregulates transcription of DAF-16 counterbalancing hyperactivation of the PI3K pathway in *daf-18/PTEN* mutants. Another potential mechanism for the effect of βHB involves the inhibition of the insulin signaling pathway. In mammals, the administration of βHB downregulates the insulin signaling in muscle (Yamada, Zhang et al., 2010). Moreover, several reports have shown that βHB administration reduces phosphorylation and activity of Akt/protein kinase downstream of the insulin receptor (Kim, Park et al., 2019, McDaniel, Rensing et al., 2011). In *C. elegans*, inhibition of AKT-1 activates DAF-16 (Hertweck, Gobel et al., 2004). Although understanding the mechanism behind βHB's action will require further studies, our results demonstrate that this ketone body positively modulates DAF-16/FOXO during neuronal development.

Multiple reports, from *C. elegans* to mammals, suggest that there is a sensitive period, typically early in development, where pharmacological or genetic interventions are more effective in ameliorating the consequences of neurodevelopmental defects (Meredith, 2015). However, recent evidence shows that phenotypes associated with certain neurodevelopmental defects can be ameliorated by interventions during adulthood (Kepler, McDiarmid et al., 2022). Our results show that βHB can rescue the phenotypic defects of *daf-18* mutants only when exposure occurs during an early critical period. The inefficacy of βHB at later developmental stages suggests that the activity of this protein during early larval stages is essential for the development and function of GABAergic motor neurons. In addition, the fact that lifelong exposure to this ketone body is not necessary to ameliorate *daf-18* mutant defects suggests that the role of DAF-16 in the maintenance of GABAergic functionality is not as relevant.

Since the PI3K/Akt pathway is highly conserved in animals, this study provides universally relevant information on how alterations in this pathway lead to neurodevelopmental defects and the mechanisms underlying the positive effects of ketogenic diets on neuronal disorders characterized by E/I imbalance.

Materials and methods

***C. elegans* culture and maintenance.** All *C. elegans* strains were grown at room temperature (20ºC) on nematode growth media (NGM) agar plates with OP50 *Escherichia coli* as a food source. The wild-type reference strain used in this study is N2 Bristol. Some of the strains were obtained through the *Caenorhabditis* Genetics Center (CGC, University of Minnesota). Worm population density was maintained low throughout their development and during the assays.

Transgenic strains were generated by microinjection of plasmid DNA containing the construct *Punc-47::daf-18cDNA* (kindly provided by Alexandra Byrne, UMASS Chan Medical School) at 20 ng/µL into the germ line of (*daf-18 (ok480); lin-15 (n765ts*)) double mutants with the co-injection marker *lin-15* rescuing plasmid pL15EK (80 ng/µl). At least three independent transgenic lines were obtained. Data are shown from a single representative line.

The strains used in this manuscript were:

CB156 *unc-25(e156*) III

MT6201 *unc-47(n2409*) III

CB1375 *daf-18(e1375*) IV

OAR144 *daf-18(ok480*) IV

GR1307 *daf-16(mgdf50)* I

OAR115 *daf-16(mgDf50);daf-18(ok480)*

OAR161 *daf-18(ok480)*; *Punc-47::daf-18*

LX929 *vsIs48 (Punc-17::GFP)*

IZ629 *ufIs34 (Punc-47::mCherry)*

OAR117 *ufis34 (Punc-47::mCherry);daf-18(ok480)*

OAR118 *vsIs48 (Punc-17::GFP); daf-18(ok480)*

OAR142 *ufis34 (Punc-47::mCherry); daf-16(mgDf50)*

OAR143 *ufis34 (Punc-47::mCherry); daf-16(mgDf50), daf-18(ok480)*

CF1553 *muIs84 [(pAD76) Psod-3::GFP + rol-6(su1006)]*

OAR140 *muIs84 [(pAD76) Psod-3::GFP + rol-6]; daf-18(ok480)*

OAR141 *muIs84 [(pAD76) Psod-3::GFP + rol-6]; daf-16(mgDf50)*

OH99 *mglS18[Pttx-3::gfp]*

OAR83 *daf-18(ok480); mglS18[Pttx-3::gfp]*

MT13471 *[Ptph-1::gfp]*

OAR112 *[Ptph-1::gfp]; daf-18(ok480)*

Paralysis assays. Paralysis assays were carried out in standard NGM plates with 2 mM aldicarb (Sigma-Aldrich) or 0.5 mM levamisole (Alfa Aesar). 25-30 L4 worms were transferred to each plate and the number of paralyzed animals were counted every 15 minutes. An animal was considered as paralyzed when it did not respond after prodding three times with a platinum wire on the head and tail (Blanco, Vela Gurovic et al., 2018).

Escape response. Escape response assays were performed on NGM agar plates seeded with a thin bacterial lawn of OP50 *E. coli.* To maintain tight control of growth and moisture, 120 μL of bacteria were seeded 24 hours before the assay and grown overnight at 37º C. The day of the assay, L4 worms were transferred to the plates and allowed to acclimate for at least 5 min. Omega turns were induced by gentle anterior touch with fine eyebrow hair and were classified as closed when the worm touched the tail with its head as previously described (Donnelly et al., 2013).

Body length assays. Body length measurements were performed in standard NGM agar plates without bacteria. L4 synchronized worms were transferred into the plates and allowed to acclimate for at least 5 min. Worms were recorded with a Amscope Mu300 camera. Animal body length, before and after touching with a platinum pick, were measured using FIJI Image J software.

Commissure analysis. Synchronized L1 or L4 animals carrying the fluorescence reporters *vsIs48* (*Punc-17::GFP*, cholinergic neurons) or *ufIs34* (*Punc-47::mCherry*, GABAergic neurons) were immobilized with sodium azide (0.25 M) on 2% agarose pads. Commissures of GABAergic and cholinergic neurons were scored with a Nikon Eclipse TE 2000 fluorescence microscope. A commissure is generally composed of a single process, and occasionally two neurites that extend together dorsally. Defects on commissures, including guidance defects, abnormal branching, and incomplete commissures were classified similar to previous reports (Oliver et al., 2019). Percentage of animals with at least one commissure defect was calculated for each neuronal class (e.g., cholinergic or GABAergic). At least 20 animals were analyzed for each individual experiment. Representative images shown in figures were collected using laser confocal microscopy (ZEISS LSM 900 with AirScan II) with 20× and 63× objectives.

β-Hydroxybutyrate assays. Worms were exposed to βHB in NGM agar plates with 20 mM DL-3-Hydroxybutyric acid sodium salt (Acros Organics). Exposure time varied in each trial as indicated.

***sod-3* expression.** *sod-3* expression levels were analyzed in transgenic strains containing the transcriptional reporter *muIs84*, as described previously (Andersen, Veuthey et al., 2022, De Rosa, Veuthey et al., 2019). Synchronized L4 animals were anesthetized with Sodium Azide (0.25 M) and mounted on 2% agarose pads. Images were collected using a Nikon Eclipse TE 2000 fluorescence microscope. GFP fluorescence intensity was quantified in same-sized ROIs

428 at the head of the animal using Image J FIJI software. Results were normalized to control
429 conditions (wild-type individuals without βHB).

430 **Statistical Analysis.** The results presented in each figure are the average of at least three
431 independent assays. Bars represent mean ± SEM. Comparison between two groups was
432 carried out using Student's *t*-test, while differences among more than two groups were carried
433 out by One-way analysis of variance (ANOVA). ns $p > 0.05$; * $p \leq 0.05$; ** $p \leq 0.01$; *** $p \leq 0.001$;
434 **** $p \leq 0.0001$. We used the software GraphPad Prism version 6.01 to perform statistics. Other
435 statistical information and the number of worms used in each assay are indicated in the figure
436 legends. For all assays, the scoring was done blinded.

437

438 **References**

439 Altun Z, Hall D (2011) Nervous system, general description. *WormAtlas doi* 10: 103-116
440 Andersen N, Veuthey T, Blanco MG, Silbestri GF, Rayes D, De Rosa MJ (2022) 1-Mesityl-3-(3-
441 Sulfonatopropyl) Imidazolium Protects Against Oxidative Stress and Delays Proteotoxicity in C. elegans.
442 *Front Pharmacol* 13: 908696
443 Arden KC (2008) FOXO animal models reveal a variety of diverse roles for FOXO transcription factors.
444 *Oncogene* 27: 2345-50
445 Baran R, Castelblanco L, Tang G, Shapiro I, Goncharov A, Jin Y (2010) Motor neuron synapse and axon
446 defects in a C. elegans alpha-tubulin mutant. *PLoS One* 5: e9655
447 Blanco MG, Vela Gurovic MS, Silbestri GF, Garelli A, Giunti S, Rayes D, De Rosa MJ (2018)
448 Diisopropylphenyl-imidazole (DII): A new compound that exerts anthelmintic activity through novel
449 molecular mechanisms. *PLoS Negl Trop Dis* 12: e0007021
450 Bozzi Y, Provenzano G, Casarosa S (2018) Neurobiological bases of autism-epilepsy comorbidity: a focus
451 on excitation/inhibition imbalance. *Eur J Neurosci* 47: 534-548
452 Butler MG, Dasouki MJ, Zhou XP, Talebizadeh Z, Brown M, Takahashi TN, Miles JH, Wang CH, Stratton R,
453 Pilarski R, Eng C (2005) Subset of individuals with autism spectrum disorders and extreme macrocephaly
454 associated with germline PTEN tumour suppressor gene mutations. *J Med Genet* 42: 318-21
455 Byrne AB, McWhirter RD, Sekine Y, Strittmatter SM, Miller DM, Hammarlund M (2016) Inhibiting
456 poly(ADP-ribosylation) improves axon regeneration. *Elife* 5
457 Byrne AB, Walradt T, Gardner KE, Hubbert A, Reinke V, Hammarlund M (2014) Insulin/IGF1 signaling
458 inhibits age-dependent axon regeneration. *Neuron* 81: 561-73
459 Caceres Ide C, Valmas N, Hilliard MA, Lu H (2012) Laterally orienting C. elegans using geometry at
460 microscale for high-throughput visual screens in neurodegeneration and neuronal development studies.
461 *PLoS One* 7: e35037
462 Calderon N, Betancourt L, Hernandez L, Rada P (2017) A ketogenic diet modifies glutamate, gamma-
463 aminobutyric acid and agmatine levels in the hippocampus of rats: A microdialysis study. *Neurosci Lett*
464 642: 158-162

465 Cantello R, Varrasi C, Tarletti R, Cecchin M, D'Andrea F, Veggiotti P, Bellomo G, Monaco F (2007)
466 Ketogenic diet: electrophysiological effects on the normal human cortex. *Epilepsia* 48: 1756-1763
467 Castro K, Baronio D, Perry IS, Riesgo RDS, Gottfried C (2017) The effect of ketogenic diet in an animal
468 model of autism induced by prenatal exposure to valproic acid. *Nutritional neuroscience* 20: 343-350
469 Christensen R, de la Torre-Ubieta L, Bonni A, Colon-Ramos DA (2011) A conserved PTEN/FOXO pathway
470 regulates neuronal morphology during C. elegans development. *Development* 138: 5257-67
471 Coghlan S, Horder J, Inkster B, Mendez MA, Murphy DG, Nutt DJ (2012) GABA system dysfunction in
472 autism and related disorders: from synapse to symptoms. *Neurosci Biobehav Rev* 36: 2044-55
473 Collier JJ, Guissart C, Olahova M, Sasorith S, Piron-Prunier F, Suomi F, Zhang D, Martinez-Lopez N,
474 Leboucq N, Bahr A, Azzarello-Burri S, Reich S, Schols L, Polvikoski TM, Meyer P, Larrieu L, Schaefer AM,
475 Alsaif HS, Alyamani S, Zuchner S et al. (2021) Developmental Consequences of Defective ATG7-Mediated
476 Autophagy in Humans. *N Engl J Med* 384: 2406-2417
477 Cupolillo D, Hoxha E, Faralli A, De Luca A, Rossi F, Tempia F, Carulli D (2016) Autistic-Like Traits and
478 Cerebellar Dysfunction in Purkinje Cell PTEN Knock-Out Mice. *Neuropsychopharmacology* 41: 1457-66
479 D'Andrea Meira I, Romao TT, Pires do Prado HJ, Kruger LT, Pires MEP, da Conceicao PO (2019) Ketogenic
480 Diet and Epilepsy: What We Know So Far. *Front Neurosci* 13: 5
481 de la Torre-Ubieta L, Bonni A (2011) Transcriptional regulation of neuronal polarity and morphogenesis
482 in the mammalian brain. *Neuron* 72: 22-40
483 De Rosa MJ, Veuthey T, Florman J, Grant J, Blanco MG, Andersen N, Donnelly J, Rayes D, Alkema MJ
484 (2019) The flight response impairs cytoprotective mechanisms by activating the insulin pathway. *Nature*
485 573: 135-138
486 Donnelly JL, Clark CM, Leifer AM, Pirri JK, Haburcak M, Francis MM, Samuel AD, Alkema MJ (2013)
487 Monoaminergic orchestration of motor programs in a complex C. elegans behavior. *PLoS Biol* 11:
488 e1001529
489 Edwards C, Canfield J, Copes N, Rehan M, Lipps D, Bradshaw PC (2014) D-beta-hydroxybutyrate extends
490 lifespan in C. elegans. *Aging* 6: 621-44
491 Gogolla N, Leblanc JJ, Quast KB, Sudhof TC, Fagiolini M, Hensch TK (2009) Common circuit defect of
492 excitatory-inhibitory balance in mouse models of autism. *J Neurodev Disord* 1: 172-81
493 Hedgecock EM, Culotti JG, Hall DH, Stern BD (1987) Genetics of cell and axon migrations in
494 Caenorhabditis elegans. *Development* 100: 365-82
495 Hertweck M, Gobel C, Baumeister R (2004) C. elegans SGK-1 is the critical component in the Akt/PKB
496 kinase complex to control stress response and life span. *Dev Cell* 6: 577-88
497 Huang YC, Pirri JK, Rayes D, Gao S, Mulcahy B, Grant J, Saheki Y, Francis MM, Zhen M, Alkema MJ (2019)
498 Gain-of-function mutations in the UNC-2/CaV2alpha channel lead to excitation-dominant synaptic
499 transmission in Caenorhabditis elegans. *Elife* 8
500 Kennedy LM, Pham SC, Grishok A (2013) Nonautonomous regulation of neuronal migration by insulin
501 signaling, DAF-16/FOXO, and PAK-1. *Cell Rep* 4: 996-1009
502 Kepler LD, McDiarmid TA, Rankin CH (2022) Rapid assessment of the temporal function and phenotypic
503 reversibility of neurodevelopmental disorder risk genes in Caenorhabditis elegans. *Disease models &*
504 *mechanisms* 15
505 Khundrakpam BS, Lewis JD, Kostopoulos P, Carbonell F, Evans AC (2017) Cortical Thickness Abnormalities
506 in Autism Spectrum Disorders Through Late Childhood, Adolescence, and Adulthood: A Large-Scale MRI
507 Study. *Cereb Cortex* 27: 1721-1731
508 Kim DH, Park MH, Ha S, Bang EJ, Lee Y, Lee AK, Lee J, Yu BP, Chung HY (2019) Anti-inflammatory action
509 of beta-hydroxybutyrate via modulation of PGC-1alpha and FoxO1, mimicking calorie restriction. *Aging*
510 11: 1283-1304
511 Kwon CH, Luikart BW, Powell CM, Zhou J, Matheny SA, Zhang W, Li Y, Baker SJ, Parada LF (2006) Pten
512 regulates neuronal arborization and social interaction in mice. *Neuron* 50: 377-88

513 Lambrechts DA, de Kinderen RJ, Vles JS, de Louw AJ, Aldenkamp AP, Majoie HJ (2017) A randomized
514 controlled trial of the ketogenic diet in refractory childhood epilepsy. *Acta Neurol Scand* 135: 231-239
515 Lee E, Lee J, Kim E (2017) Excitation/Inhibition Imbalance in Animal Models of Autism Spectrum
516 Disorders. *Biol Psychiatry* 81: 838-847
517 Li J, Yen C, Liaw D, Podsypanina K, Bose S, Wang SI, Puc J, Miliaresis C, Rodgers L, McCombie R, Bigner
518 SH, Giovanella BC, Ittmann M, Tycko B, Hibshoosh H, Wigler MH, Parsons R (1997) PTEN, a putative
519 protein tyrosine phosphatase gene mutated in human brain, breast, and prostate cancer. *Science* 275:
520 1943-7
521 Li Q, Liang J, Fu N, Han Y, Qin J (2021) A Ketogenic Diet and the Treatment of Autism Spectrum Disorder.
522 *Frontiers in pediatrics* 9: 650624
523 Maehama T, Dixon JE (1998) The tumor suppressor, PTEN/MMAC1, dephosphorylates the lipid second
524 messenger, phosphatidylinositol 3,4,5-trisphosphate. *J Biol Chem* 273: 13375-8
525 Maglioni S, Schiavi A, Melcher M, Brinkmann V, Luo Z, Laromaine A, Raimundo N, Meyer JN, Distelmaier
526 F, Ventura N (2022) Neuroligin-mediated neurodevelopmental defects are induced by mitochondrial
527 dysfunction and prevented by lutein in C. elegans. *Nat Commun* 13: 2620
528 McDaniel SS, Rensing NR, Thio LL, Yamada KA, Wong M (2011) The ketogenic diet inhibits the
529 mammalian target of rapamycin (mTOR) pathway. *Epilepsia* 52: e7-11
530 McIntire SL, Jorgensen E, Kaplan J, Horvitz HR (1993) The GABAergic nervous system of Caenorhabditis
531 elegans. *Nature* 364: 337-341
532 Meredith RM (2015) Sensitive and critical periods during neurotypical and aberrant neurodevelopment:
533 a framework for neurodevelopmental disorders. *Neurosci Biobehav Rev* 50: 180-8
534 Mihaylova VT, Borland CZ, Manjarrez L, Stern MJ, Sun H (1999) The PTEN tumor suppressor homolog in
535 Caenorhabditis elegans regulates longevity and dauer formation in an insulin receptor-like signaling
536 pathway. *Proc Natl Acad Sci U S A* 96: 7427-32
537 Moreno-Layseca P, Streuli CH (2014) Signalling pathways linking integrins with cell cycle progression.
538 *Matrix Biol* 34: 144-53
539 Neal EG, Chaffe H, Schwartz RH, Lawson MS, Edwards N, Fitzsimmons G, Whitney A, Cross JH (2008) The
540 ketogenic diet for the treatment of childhood epilepsy: a randomised controlled trial. *The Lancet*
541 *Neurology* 7: 500-6
542 Newman JC, Verdin E (2017) beta-Hydroxybutyrate: A Signaling Metabolite. *Annu Rev Nutr* 37: 51-76
543 Oblak A, Gibbs TT, Blatt GJ (2009) Decreased GABAA receptors and benzodiazepine binding sites in the
544 anterior cingulate cortex in autism. *Autism Res* 2: 205-19
545 Ogg S, Ruvkun G (1998) The C. elegans PTEN homolog, DAF-18, acts in the insulin receptor-like metabolic
546 signaling pathway. *Molecular cell* 2: 887-93
547 Oliver D, Norman E, Bates H, Avard R, Rettler M, Benard CY, Francis MM, Lemons ML (2019) Integrins
548 Have Cell-Type-Specific Roles in the Development of Motor Neuron Connectivity. *J Dev Biol* 7
549 Paik JH, Ding Z, Narurkar R, Ramkissoon S, Muller F, Kamoun WS, Chae SS, Zheng H, Ying H, Mahoney J,
550 Hiller D, Jiang S, Protopopov A, Wong WH, Chin L, Ligon KL, DePinho RA (2009) FoxOs cooperatively
551 regulate diverse pathways governing neural stem cell homeostasis. *Cell Stem Cell* 5: 540-53
552 Palmisano NJ, Melendez A (2019) Autophagy in C. elegans development. *Dev Biol* 447: 103-125
553 Paradis S, Ruvkun G (1998) Caenorhabditis elegans Akt/PKB transduces insulin receptor-like signals from
554 AGE-1 PI3 kinase to the DAF-16 transcription factor. *Genes Dev* 12: 2488-98
555 Park J, Lee K, Kim K, Yi SJ (2022) The role of histone modifications: from neurodevelopment to
556 neurodiseases. *Signal Transduct Target Ther* 7: 217
557 Petersen SC, Watson JD, Richmond JE, Sarov M, Walthall WW, Miller DM, III (2011) A transcriptional
558 program promotes remodeling of GABAergic synapses in Caenorhabditis elegans. *J Neurosci* 31: 15362-
559 15375
560 Pirri JK, Alkema MJ (2012) The neuroethology of C. elegans escape. *Curr Opin Neurobiol* 22: 187-193

561 Rademacher S, Eickholt BJ (2019) PTEN in Autism and Neurodevelopmental Disorders. *Cold Spring Harb*
562 *Perspect Med* 9
563 Radu A, Neubauer V, Akagi T, Hanafusa H, Georgescu MM (2003) PTEN induces cell cycle arrest by
564 decreasing the level and nuclear localization of cyclin D1. *Mol Cell Biol* 23: 6139-49
565 Rubenstein JL, Merzenich MM (2003) Model of autism: increased ratio of excitation/inhibition in key
566 neural systems. *Genes Brain Behav* 2: 255-67
567 Safdie G, Liewald JF, Kagan S, Battat E, Gottschalk A, Treinin M (2016) RIC-3 phosphorylation enables
568 dual regulation of excitation and inhibition of Caenorhabditis elegans muscle. *Mol Biol Cell* 27: 2994-
569 3003
570 Santo EE, Paik J (2018) FOXO in Neural Cells and Diseases of the Nervous System. *Curr Top Dev Biol* 127:
571 105-118
572 Sato K, Sato M, Audhya A, Oegema K, Schweinsberg P, Grant BD (2006) Dynamic regulation of caveolin-1
573 trafficking in the germ line and embryo of Caenorhabditis elegans. *Mol Biol Cell* 17: 3085-94
574 Schaffner I, Minakaki G, Khan MA, Balta EA, Schlotzer-Schrehardt U, Schwarz TJ, Beckervordersandforth
575 R, Winner B, Webb AE, DePinho RA, Paik J, Wurst W, Klucken J, Lie DC (2018) FoxO Function Is Essential
576 for Maintenance of Autophagic Flux and Neuronal Morphogenesis in Adult Neurogenesis. *Neuron* 99:
577 1188-1203 e6
578 Shimazu T, Hirschey MD, Newman J, He W, Shirakawa K, Le Moan N, Grueter CA, Lim H, Saunders LR,
579 Stevens RD, Newgard CB, Farese RV, Jr., de Cabo R, Ulrich S, Akassoglou K, Verdin E (2013) Suppression
580 of oxidative stress by beta-hydroxybutyrate, an endogenous histone deacetylase inhibitor. *Science* 339:
581 211-4
582 Smith GD, White J, Lugo JN (2016) Superimposing Status Epilepticus on Neuron Subset-Specific PTEN
583 Haploinsufficient and Wild Type Mice Results in Long-term Changes in Behavior. *Sci Rep* 6: 36559
584 Stavoe AK, Hill SE, Hall DH, Colon-Ramos DA (2016) KIF1A/UNC-104 Transports ATG-9 to Regulate
585 Neurodevelopment and Autophagy at Synapses. *Dev Cell* 38: 171-85
586 Stawicki TM, Zhou K, Yochem J, Chen L, Jin Y (2011) TRPM channels modulate epileptic-like convulsions
587 via systemic ion homeostasis. *Current biology : CB* 21: 883-8
588 Tao HW, Li YT, Zhang LI (2014) Formation of excitation-inhibition balance: inhibition listens and changes
589 its tune. *Trends Neurosci* 37: 528-30
590 van Diepen MT, Eickholt BJ (2008) Function of PTEN during the formation and maintenance of neuronal
591 circuits in the brain. *Developmental neuroscience* 30: 59-64
592 Vashlishan AB, Madison JM, Dybbs M, Bai J, Sieburth D, Ch'ng Q, Tavazoie M, Kaplan JM (2008) An RNAi
593 screen identifies genes that regulate GABA synapses. *Neuron* 58: 346-61
594 Verpeut JL, DiCicco-Bloom E, Bello NT (2016) Ketogenic diet exposure during the juvenile period
595 increases social behaviors and forebrain neural activation in adult Engrailed 2 null mice. *Physiol Behav*
596 161: 90-98
597 White JG, Albertson DG, Anness MA (1978) Connectivity changes in a class of motoneurone during the
598 development of a nematode. *Nature* 271: 764-6
599 White JG, Southgate E, Thomson JN, Brenner S (1986) The structure of the nervous system of the
600 nematode Caenorhabditis elegans. *Philos Trans R Soc Lond B Biol Sci* 314: 1-340
601 Wu X, Reddy DS (2012) Integrins as receptor targets for neurological disorders. *Pharmacol Ther* 134: 68-
602 81
603 Xia S, Zhou Z, Jia Z (2018) PAK1 regulates inhibitory synaptic function via a novel mechanism mediated
604 by endocannabinoids. *Small GTPases* 9: 322-326
605 Yamada T, Zhang SJ, Westerblad H, Katz A (2010) beta-Hydroxybutyrate inhibits insulin-mediated
606 glucose transport in mouse oxidative muscle. *Am J Physiol Endocrinol Metab* 299: E364-73
607 Yudkoff M, Daikhin Y, Horyn O, Nissim I, Nissim I (2008) Ketosis and brain handling of glutamate,
608 glutamine, and GABA. *Epilepsia* 49 Suppl 8: 73-5

609 Zhou X, Bessereau JL (2019) Molecular Architecture of Genetically-Tractable GABA Synapses in C.
610 elegans. *Front Mol Neurosci* 12: 304

611

612

Acknowledgments

Some strains were provided by the CGC, which is funded by NIH Office of Research Infrastructure Programs (P40 OD010440). We thank Mark Alkema and Alex Byrne for strains and technical support. We like to thank Andrés Garelli, Guillermo Spitzmaul, Gabriela Salvador, Mark Alkema, Inés Carrera and Claire Bénard for helpful discussions.

Funding

This work was supported by Grants from: 1) Consejo Nacional de Investigaciones Científicas y Técnicas, Argentina to INIBIBB (PUE- N22920170100017CO) and to DR/ MJDR (PIP No. 11220200101606CO). 2) Agencia Nacional de Promoción de la Ciencia y la Tecnología ANPCYT Argentina to DR (PICT 2019-0480 and PICT-2021-I-A-00052) and MJDR (PICT-2017-0566 and PICT-2020-1734) and 3) Universidad Nacional Del Sur to DR (PGI: 24/B291) and MJDR (PGI: 24/B261). The funders had no role in the study design, data collection, and analysis, decision to publish, or preparation of the manuscript.

Conflict of Interest

The authors declare that the research was conducted in the absence of any commercial or financial relationships that could be construed as a potential conflict of interest.

Figure Legends

Figure 1. *daf-18/PTEN* mutants exhibit phenotypes typical of GABA-deficient animals. A and B- Quantification of paralysis induced by cholinergic drugs. Assays were performed in NGM plates containing 2 mM aldicarb (A) and 0.5 mM levamisole (B). Each data point represents the mean percentage of animals paralyzed every 15 min ± SEM. At least four independent trials with 20-30 animals for each genotype were performed. C- Measurement of body length in response to anterior touch. Quantification of body shortening after touching was calculated as the decrease of body length related to the length of the animal before being touched. Between 40-55 animals for each genotype were analyzed. Data are represented as mean ± SEM. D- (Top) Scheme of *C. elegans* escape response in NGM agar. In wild-type animals, anterior gentle touch elicits an escape response in which reversals are often coupled to a closed omega turn that allows the animal to change locomotion in a direction 180° opposite to its original course. (Bottom) Quantification of closed omega turns. After eliciting the escape response by an anterior gentle touch, the omega turns were classified as closed (head and tail are in contact) or open (no contact between head and tail). The percentage of closed omega turns was calculated for each condition. At least seven independent trials with 20 animals for each genotype were performed. Results are presented as mean ± SEM. One-way analysis of variance (ANOVA) was used to test statistical differences among treatment groups in A, B and D, and Kruskal-Wallis test was used in C. Statistical significance compared to wild-type or between different strains (ns $p > 0.05$; * $p \leq 0.05$; ** $p \leq 0.01$; *** $p \leq 0.001$; **** $p \leq 0.0001$). Strains used are: OAR144 *daf-18 (ok480),* GR1307 *daf-16 (mgdf50)* and OAR115 *daf-18(ok480)*; *daf-16(mgDf50).* The strain CB156 *unc-25(e156)* was included as a strong GABA-deficient control.

Figure 2. *daf-18/PTEN* mutants show morphological defects in GABAergic, but not in cholinergic motor neurons.

A- Representative image of a wild-type animal expressing mCherry in the GABAergic motor neurons. Scale Bar is 50 μm. In the upper inset, the commissural processes can be appreciated with higher resolution. The lower inset shows a ventral view of the animal (note that all the processes travel through the right side of the animal body). In the insets, the scale bar is 25 μm. B- Representative images of commissure defects observed in *daf-18 (ok480)* mutants (arrows). Scale Bar is 25 μm. The defects shown are: Short, commissure length less than half of nematode width; Bridged, neighboring commissures linked by a neurite; Guidance, commissures that do not reach dorsal nerve cord; and Handedness, commissure running along the opposite side of the animal's body. C- Quantification of GABAergic system defects is represented by the proportion of animals with at least one incidence of each independent defect shown in B. Each bar represents the mean ± SEM for at least three trials (~20 animals per trial). One-way analysis of variance (ANOVA) was used to test statistical differences among different conditions. D- Representative images of animals expressing GFP in the cholinergic neurons. Scale bar is 50 μm. In the insets, the commissural processes can be appreciated with higher resolution (scale bar is 25 μm). E- Quantification of cholinergic system defects is represented by the proportion of animals with at least one incidence of each independent defect. Each bar represents the mean ± SEM for at least four trials (~ 20 animals per trial). Statistical significance between the strains was determined by two-tailed unpaired Student's t test. (ns $p > 0.05$; **** $p \leq 0.0001$).

A anterior; P Posterior; D Dorsal; V Ventral.

Figure 3. *daf-18/PTEN* acts autonomously to regulate GABAergic motor neuron development.

A- Quantification of closed omega turns (see legend Figure 1). B- Quantification of commissure defects in GABAergic neurons is represented as the proportion of animals with at least one defect. *daf-18(ok480); Punc-47::daf-18* animals express *daf-18* solely in GABAergic neurons Results are presented as mean ± SEM for at least four trials. One-way analysis of variance (ANOVA) was used to test statistical differences among treatment groups (ns $p > 0.05$; ** $p \leq 0,01$; *** $p \leq 0.001$; **** $p \leq 0.0001$).

Figure 4. Dietary βHB supplementation rescues GABAergic deficits in *daf-18/PTEN* mutants.

A and B- Quantification of paralysis induced by cholinergic drugs. The assays were performed in NGM plates containing 2 mM aldicarb (A) and 0.5 mM levamisole (B). Each data point represents the mean percentage of animals paralyzed every 15 min ± SEM. At least four independent trials with 25-30 animals for each condition were performed. C- Quantification of closed omega turns during the escape response. The percentage of closed omega turns was calculated for each condition. At least six independent trials with ~20 animals for each condition were performed. D- Quantification of commissure defects in GABAergic neurons is represented as the proportion of animals with at least one defect. Animals were exposed to βHB (20 mM) throughout development (from eggs to L4). At least three independent trials with ~20 animals for each condition were performed. Results are presented as mean ± SEM. Statistical significance between the conditions was determined by two-tailed unpaired Student's t test (ns $p > 0.05$; *$p \leq 0.05$). Strains used are: OAR144 *daf-18 (ok480)*, GR1307 *daf-16(mgdf50)* and OAR115 *daf-18(ok480)*; *daf-16(mgDf50).*

Figure 5. Early developmental stages are critical for βHB-modulation of GABAergic signaling.

A- Scheme of βHB exposure. Animals were exposed to βHB during different developmental intervals: from embryo to the L1 stage (E-L1), from L1 to L2 (L1-L2), from L2 to L4 (L2-L4), or throughout development (from embryo to L4, E-L4). B- Quantification of closed omega turns. The percentage of animals that performed a closed omega turn was determined for each interval of βHB exposure. C- Quantification of commissure defects in GABAergic neurons is represented as the proportion of animals with at least one defect. At least four independent trials with ~20 animals for each condition were performed. Results are presented as mean ± SEM. One-way analysis of variance (ANOVA) was used to test statistical differences among treatment groups (ns $p > 0.05$; *$p \leq 0.05$; ** $p \leq 0,01$).

Figure 6. Scheme of the neurodevelopmental consequences of *daf-18/PTEN* mutations in *C. elegans* and the effect of the ketone body KB.

(Top) In wild-type animals, the negative modulatory activity of DAF-18/PTEN on AKT-1 ensures sufficient levels of DAF-16/FOXO activation for proper GABAergic and cholinergic neurodevelopment.

(Middle) In *daf-18/PTEN* mutants, the high activity of AKT-1 and the resulting massive inactivation of DAF-16/FOXO, selectively affects the development of GABAergic neurons (without affecting the morphological development of cholinergic neurons). This leads to

730 phenotypes associated with high excitation/inhibition ratio (open omega turn during the escape
731 response).
732 (Bottom) The ketone body β-hydroxybutyrate increases FOXO activity in *daf-18/PTEN* mutants,
733 rescuing, at least partially, the defects in GABAergic neurodevelopment and the E/I imbalance.
734

Supplementary Figure Legends

Suppl. Figure 1. *daf-18/PTEN* mutants are hypersensitive to cholinergic drugs.

A- Gene structure of *daf-18*. Coding sequences are represented by blue boxes. The *daf-18(e1375)* mutant allele inserts a 30 bp sequence in exon IV. This insertion occurs downstream of the phosphatase catalytic domain and causes a frameshift that leads to premature truncation of the protein. This *e1375* mutation partially reduces DAF-18 function. The *daf-18(ok480)* allele contains a 956 bp deletion that removes most of exon 3 and exon 4 and is generally considered to be a null allele. B and C- Quantification of paralysis induced by cholinergic drugs. The assays were performed in NGM plates containing 2 mM aldicarb (A) and 0.5 mM levamisole (B). Each data point represents the mean percentage of animals paralyzed every 15 min ± SEM. At least four independent trials with 25-30 animals for each genotype were performed. One-way analysis of variance (ANOVA) was used to test statistical differences among strains (ns $p > 0.05$; * $p \leq 0.05$; ** $p \leq 0.01$; *** $p \leq 0.001$; **** $p \leq 0.0001$). Strains tested are: OAR 144 *daf-18(ok480*) and CB1375 *daf-18(e1375*). The strain CB156 *unc-25(e156)* was included as a strong GABA-deficient control.

Suppl. Figure 2. The conserved PI3K-Akt-FOXO pathway.

daf-18/PTEN encodes a lipid and protein phosphatase that hydrolyzes phosphatidylinositol (3,4,5)-trisphosphate (PIP_3) to phosphatidylinositol-4,5-bisphosphate (PIP_2). It is the main negative modulator of AKT activity. In *daf-18/PTEN* mutants, AKT-1 is overactivated leading to

high levels of DAF-16/FOXO phosphorylation that prevents the translocation of this transcription factor to the nucleus.

Suppl. Figure 3. *daf-18* mutants exhibit GABAergic commissures defects at the L1 stage.

A- Representative image of L1 animals expressing the fluorescence reporter *Punc-47::mCherry* in wild-type (Top) and *daf-18(ok480)* mutant (Bottom) backgrounds. In this earliest larval stage, only six GABAergic DD motor neurons are born and send commissures dorsally, although without forming functional synapses with the dorsal muscles. The inset shows a typical defective (branched) commissure of *daf-18* mutants. B- Quantification of GABAergic system defects in L1s is represented by the proportion of animals with at least one commissure defect. Each bar represents the mean ± SEM for a total of five independent experiments (~20 animals per experiment). Statistical significance between the strains was determined by two-tailed unpaired Student's t test. (** $p \leq 0.01$). A, anterior; P Posterior; D Dorsal; V Ventral.

Suppl. Figure 4. Exposure to βHB induces *sod-3* expression in *daf-18*, but not in *daf-16* mutants.

A- Representative fluorescence images (20X magnification) of worms expressing *Psod-3::GFP* in different genetic backgrounds (wild-type, *daf-18(ok480*) and *daf-16(mgDf50))* upon exposure to βHB (20mM). B- Corresponding quantification of the fluorescence intensity per animal in the head. Scatter dot plot (line at the median) with the relative expression of *Psod-3::GFP* normalized to naïve wild-type animals. Statistical significance between conditions was determined by Kruskal-Wallis test (ns $p > 0.05$; ** $p \leq 0.01$; **** $p \leq 0.0001$, n= 80-90).

Suppl. Figure 5. Exposure to βHB ameliorates post-prodding body shortening in *daf-18* mutants.

Measurement of body length in response to anterior touch. Quantification of body shortening after touching was calculated as the decrease of body length related to the length of the animal before being touched. Between 35-40 animals under exposure (or not) to βHB (20 mM) for each condition were analyzed. Statistical significance between the treatments was determined by Kruskal-Wallis test (ns $p > 0.05$; * $p \leq 0.05$).

Suppl. Figure 6. βHB does not prevent neurodevelopmental defects in AIY and HSN neurons.

A- AIY processes were visualized in transgenic animals expressing cytoplasmic *GFP* in AIY neurons (*Pttx-3b::GFP*) in wild-type and *daf-18(ok480)* mutant backgrounds. AIY neuronal growth defects were quantified as described before (Christensen *et al*., 2011). Left: Scheme of AIY morphology and location in the nematode nerve ring. Blue, pharynx; red, AIY interneurons. Pink: wild-type AIY morphology. The two interneurons meet at the dorsal midline. Light blue and yellow: denote different levels of AIY neurite truncation. Right: Percentage of animals with truncated neurites in wild-type and *daf-18(ok480)* mutants under exposure (or not) to βHB (20 mM). B- HSN were visualized in transgenic animals expressing *GFP* in serotonergic neurons (*Ptph-1::GFP*) in wild-type and *daf-18(ok480)* mutant backgrounds. HSN under-migration defects were identified as described before (Kennedy et al., 2013). Left: Schematic representation of the HSN migratory route during embryogenesis and the corresponding

806 location of the HSN (green circle) in a young adult animal. Only one of two bilaterally symmetric
807 HSNs is illustrated. Colors show information about the position of HSNs: Light purple: complete
808 migration (≥ 0.4), middle purple: intermediated migration (>0.2-<0.4), dark purple: unmigrated
809 (≤0.2). Right: Quantification of the percentage of animals with different HSN migration positions
810 (the most under-migrated neuron of each animal is considered). Bars represent the mean
811 values of at least three independent experiments. Note that there is no significant effect with
812 βHB treatment compare to controls.
813

Figure 1

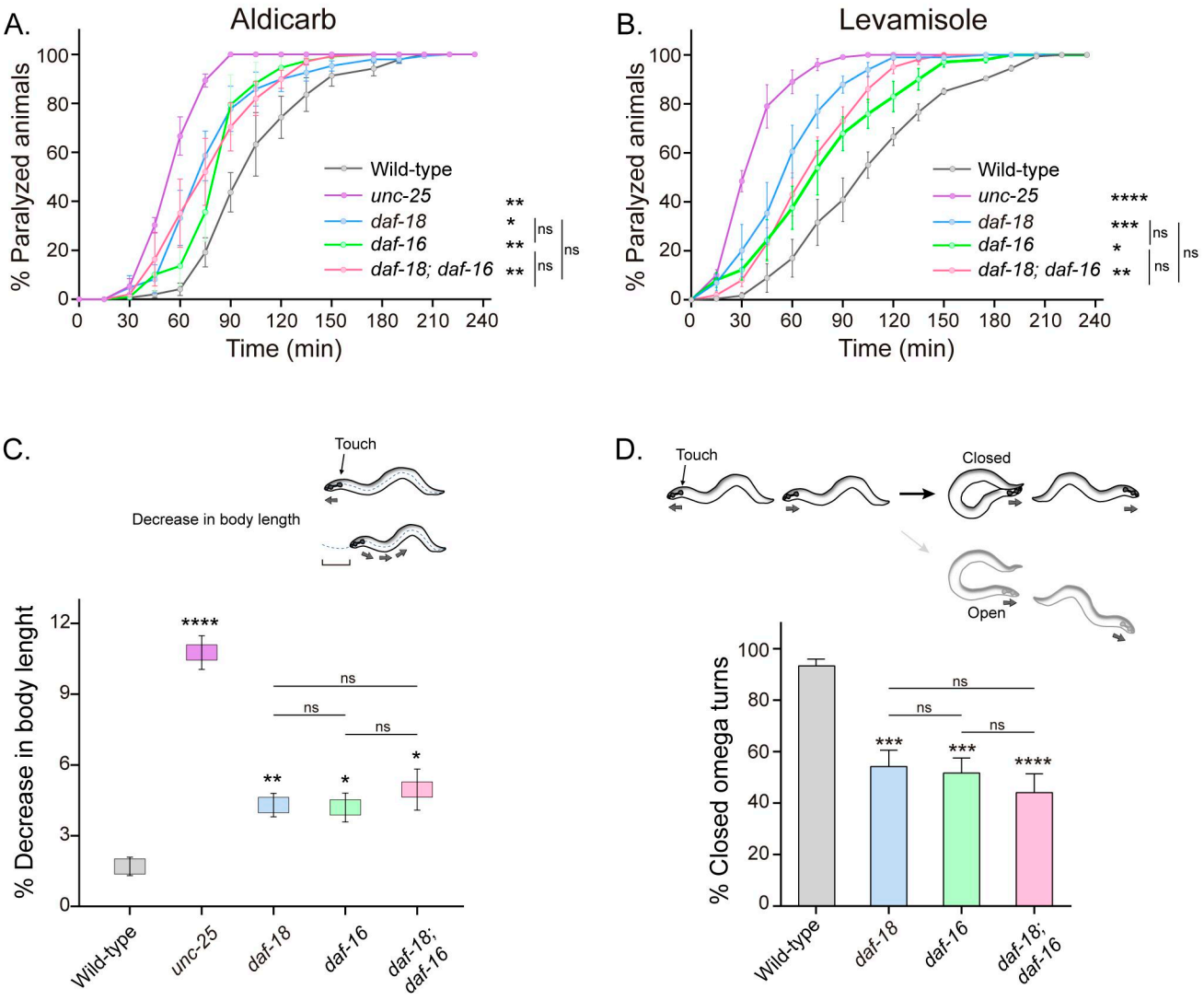
A.
Aldicarb
% Paralyzed animals
Time (min)
Wild-type
unc-25
daf-18
daf-16
daf-18; daf-16
**
*
**
**
ns
ns
ns
B.
Levamisole
% Paralyzed animals
Time (min)
Wild-type
unc-25
daf-18
daf-16
daf-18; daf-16
****
***
*
**
ns
ns
ns
C.
Touch
Decrease in body length
% Decrease in body lenght
****
**
*
*
ns
ns
ns
Wild-type
unc-25
daf-18
daf-16
daf-18; daf-16
D.
Touch
Closed
Open
% Closed omega turns
***
***
****
ns
ns
ns
Wild-type
daf-18
daf-16
daf-18; daf-16

Figure 2

A. *Punc-47*::mCherry (GABAergic neurons)

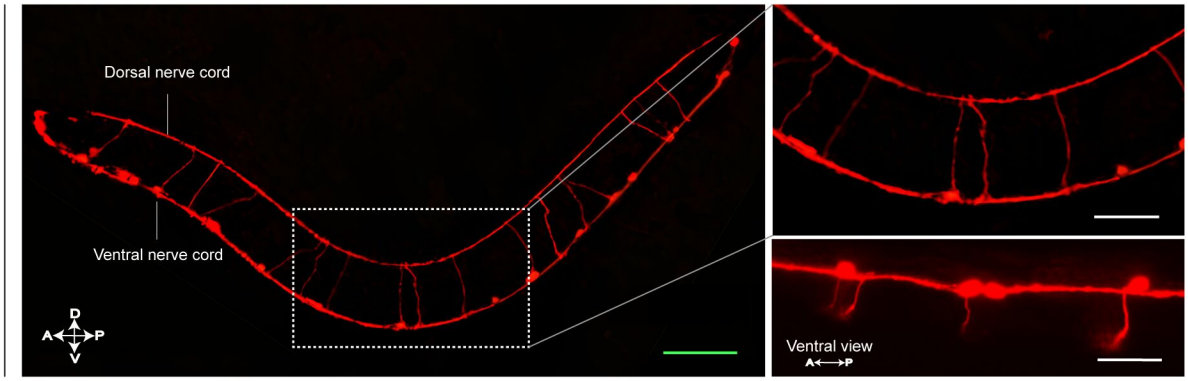

B.

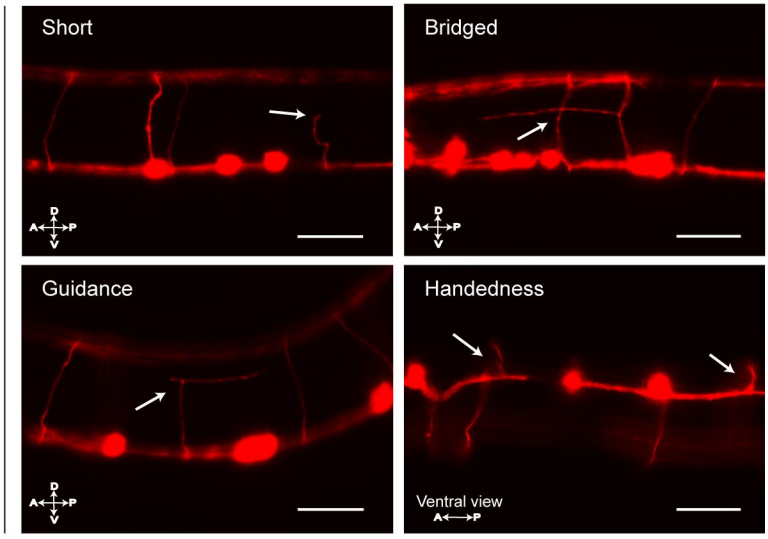

C.

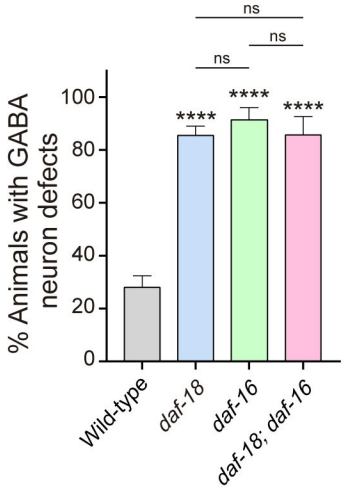

D. *Punc-17*::GFP (Cholinergic neurons)

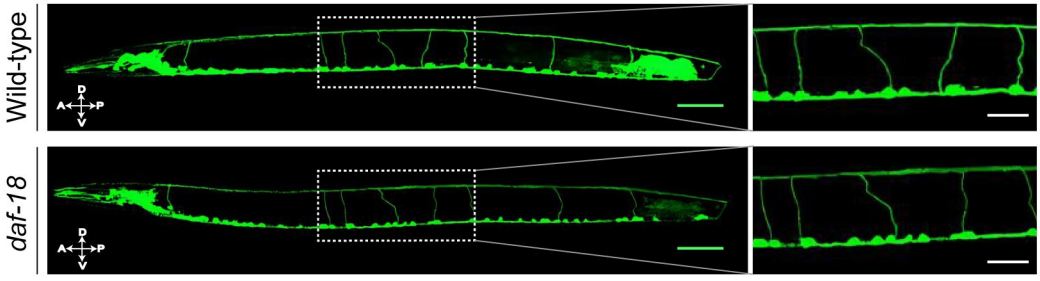

E.

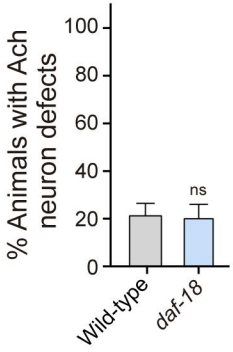

Figure 3

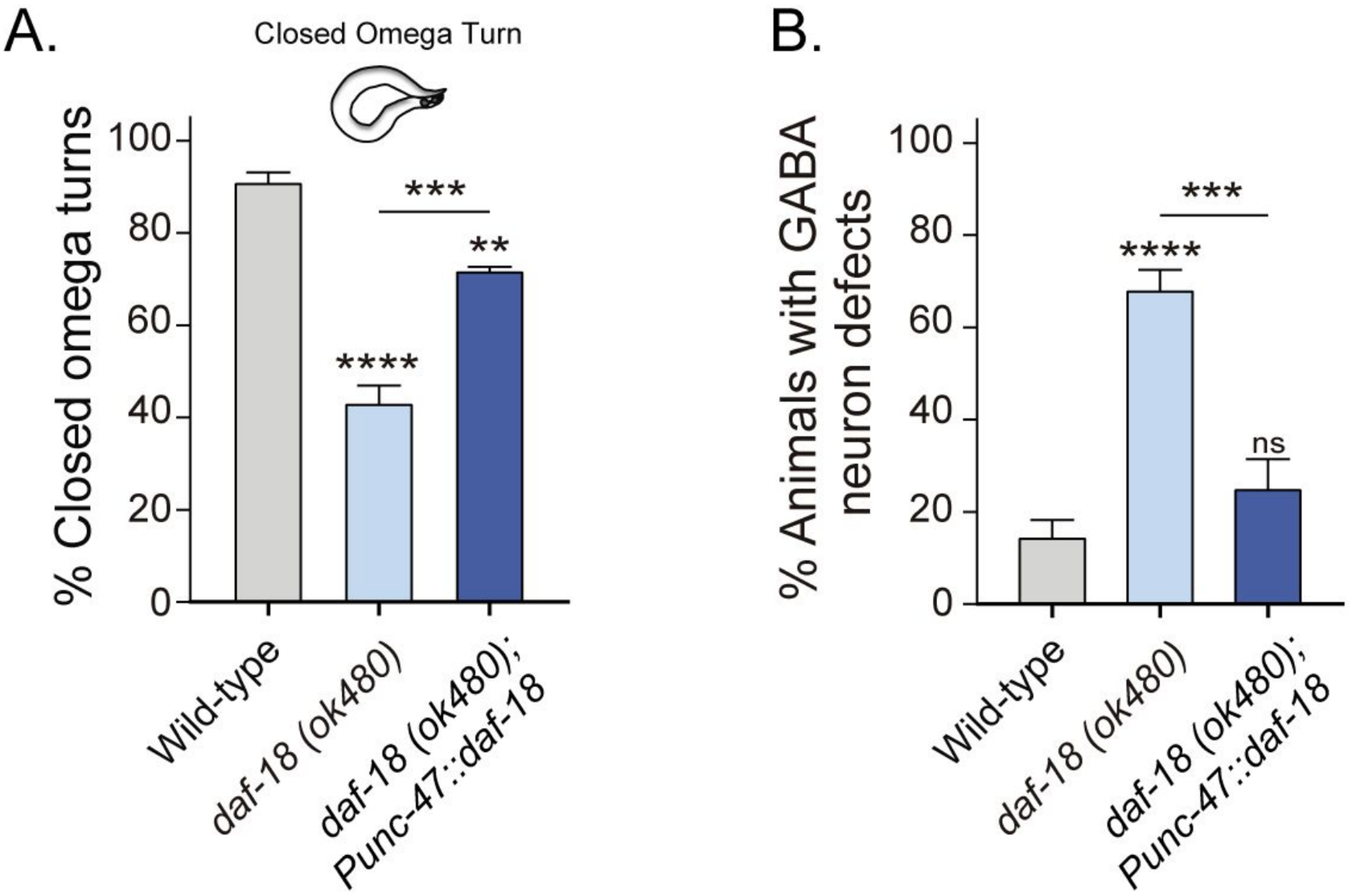
A.
Closed Omega Turn
% Closed omega turns
100
80
60
40
20
0
***
**
****
Wild-type
daf-18 (ok480)
daf-18 (ok480);
Punc-47::daf-18
B.
% Animals with GABA
neuron defects
100
80
60
40
20
0
***
****
ns
Wild-type
daf-18 (ok480)
daf-18 (ok480);
Punc-47::daf-18

Figure 4

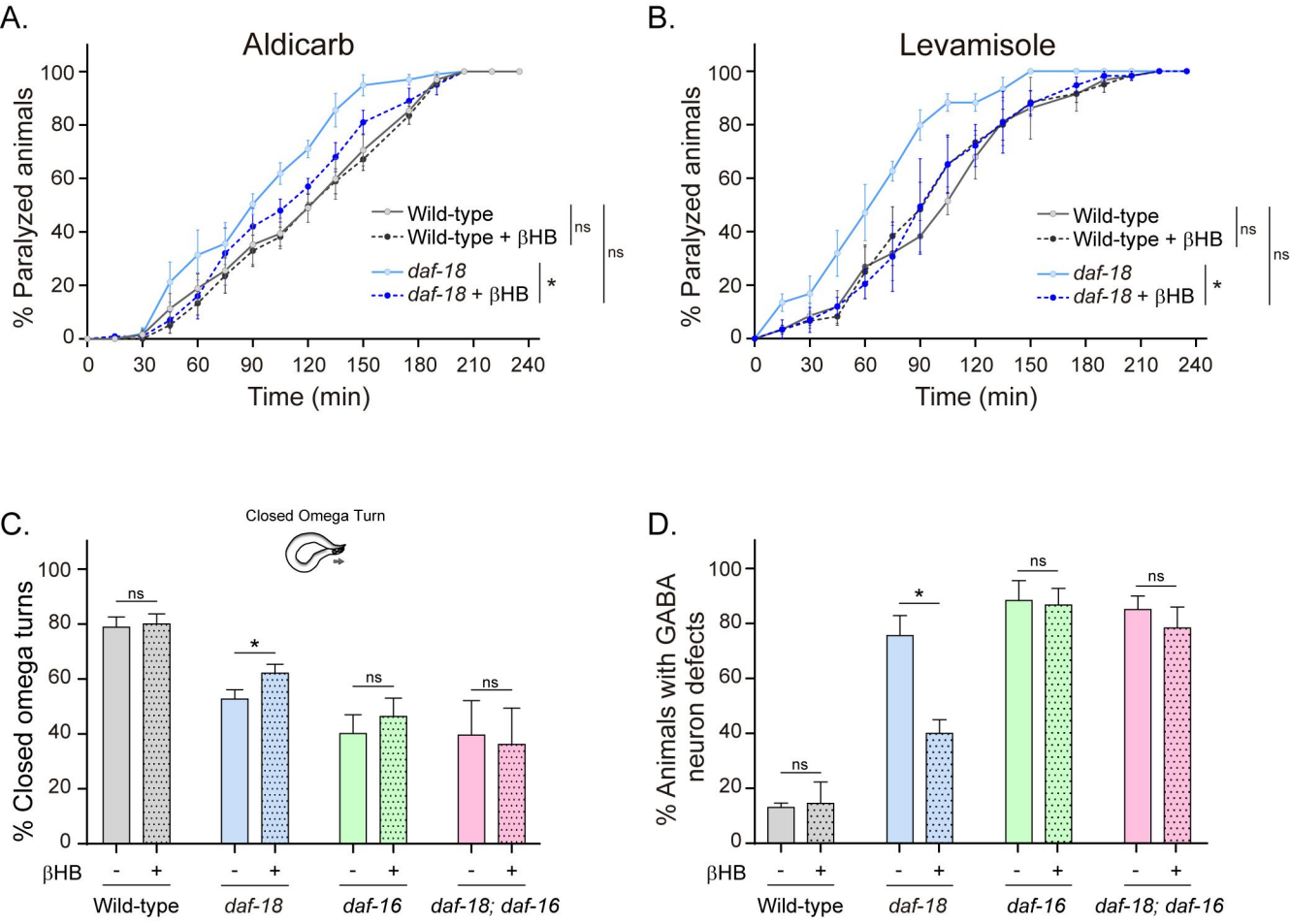
A.
Aldicarb
% Paralyzed animals
Time (min)
Wild-type
Wild-type + βHB
daf-18
daf-18 + βHB
ns
*
ns
B.
Levamisole
% Paralyzed animals
Time (min)
Wild-type
Wild-type + βHB
daf-18
daf-18 + βHB
ns
*
ns
C.
Closed Omega Turn
% Closed omega turns
βHB
Wild-type
daf-18
daf-16
daf-18; daf-16
D.
% Animals with GABA neuron defects
βHB
Wild-type
daf-18
daf-16
daf-18; daf-16

Figure 5

A.

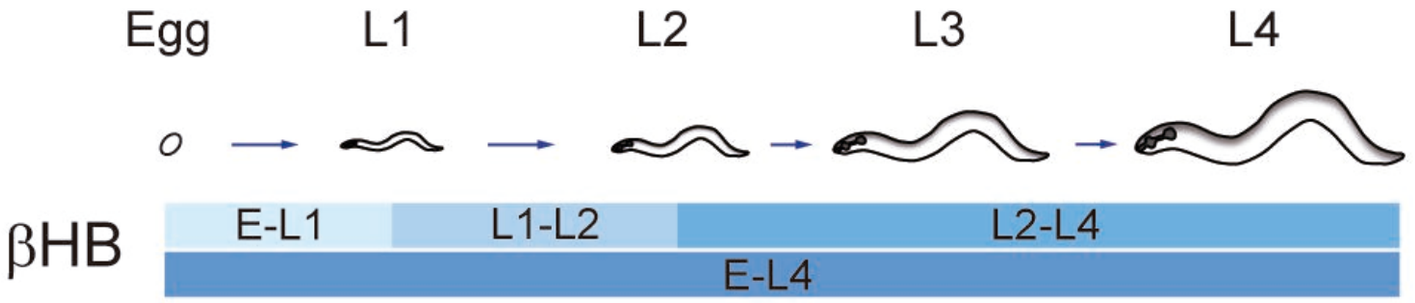
Egg
L1
L2
L3
L4
βHB
E-L1
L1-L2
L2-L4
E-L4

B.

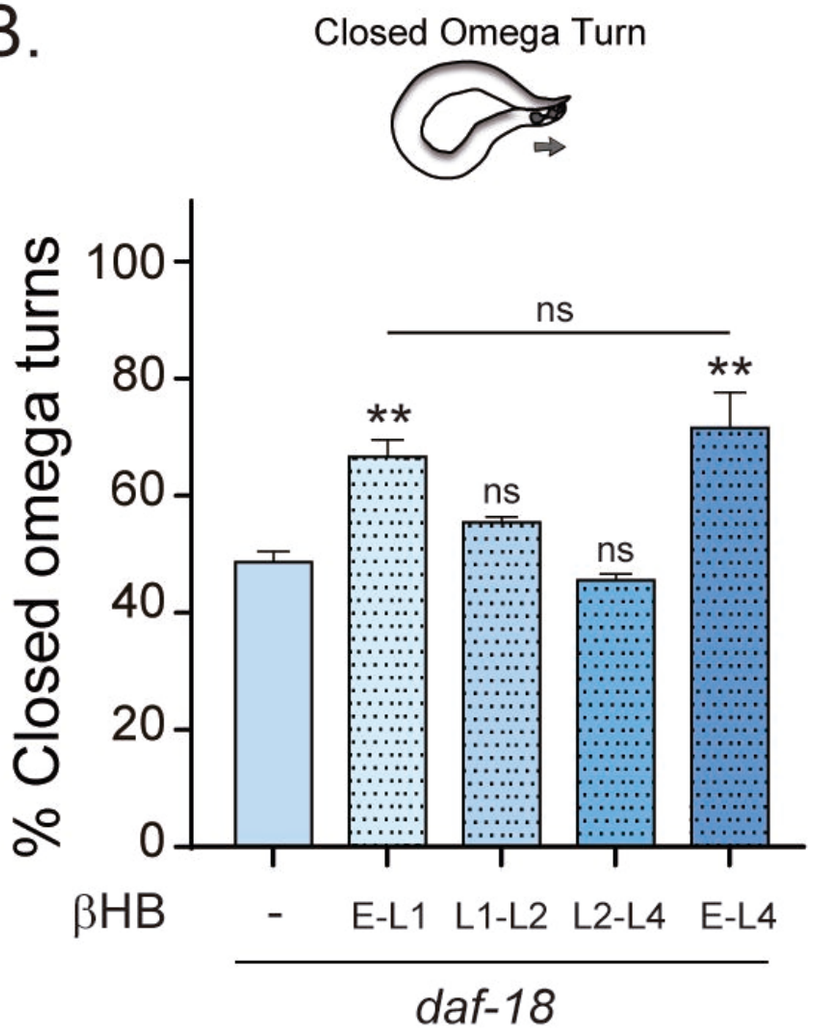
Closed Omega Turn
% Closed omega turns
100
80
60
40
20
0
ns
**
**
ns
ns
βHB
-
E-L1
L1-L2
L2-L4
E-L4
daf-18

C.

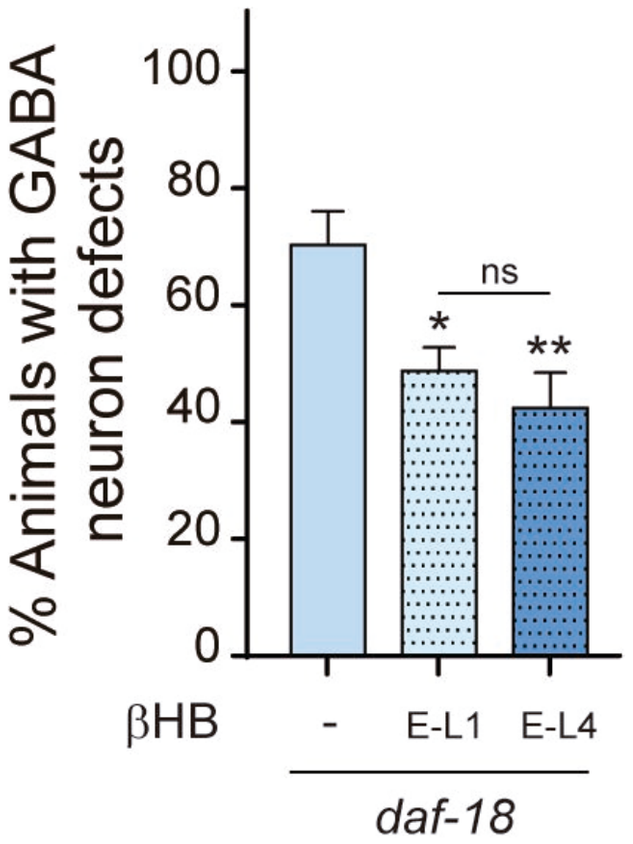
% Animals with GABA neuron defects
100
80
60
40
20
0
ns
*
**
βHB
-
E-L1
E-L4
daf-18

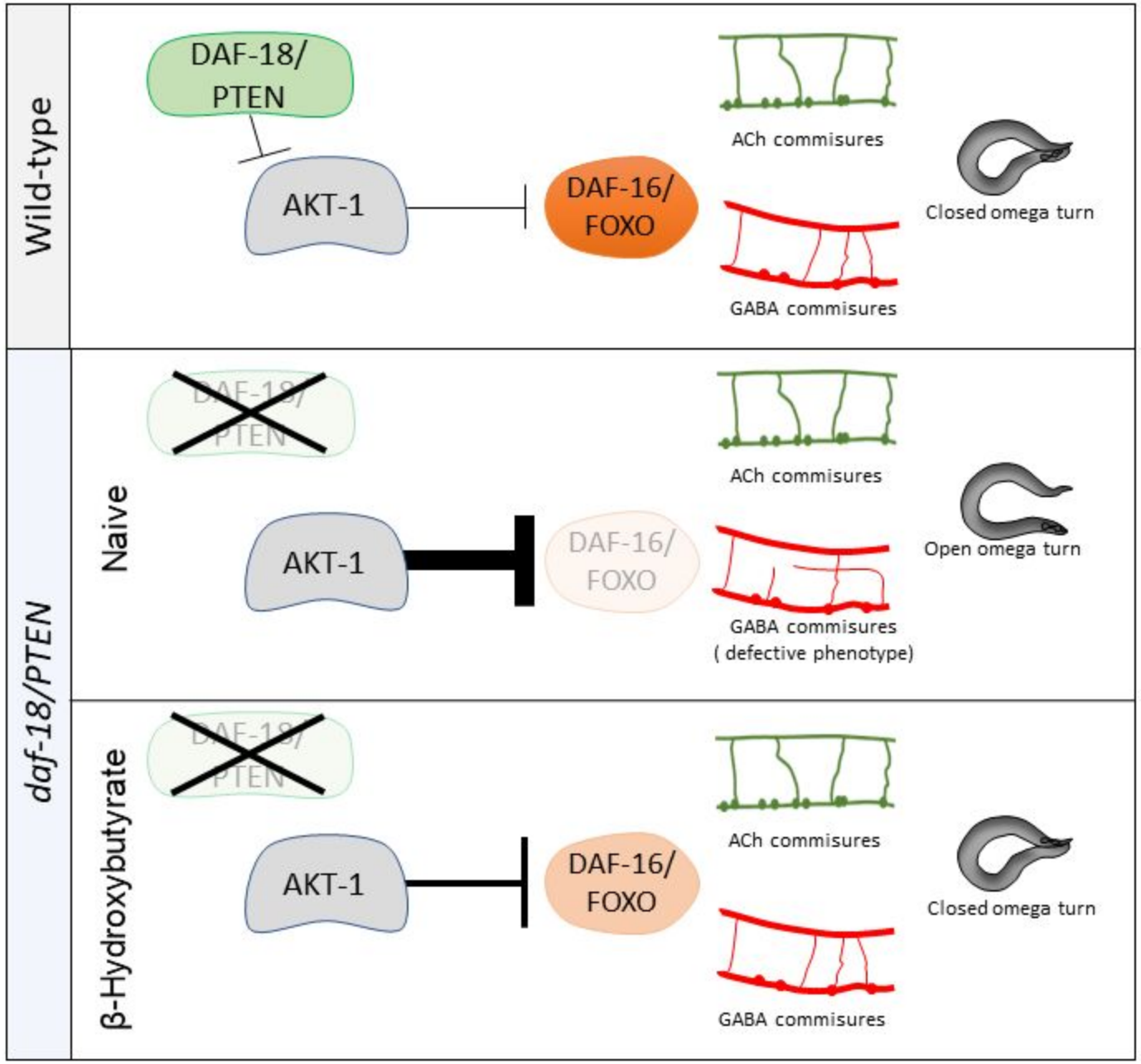
Wild-type
DAF-18/
PTEN
AKT-1
DAF-16/
FOXO
ACh commisures
GABA commisures
Closed omega turn
daf-18/PTEN
Naive
AKT-1
DAF-16/
FOXO
ACh commisures
GABA commisures
(defective phenotype)
Open omega turn
β-Hydroxybutyrate
AKT-1
DAF-16/
FOXO
ACh commisures
GABA commisures
Closed omega turn

Suppl. Figure 1

A.

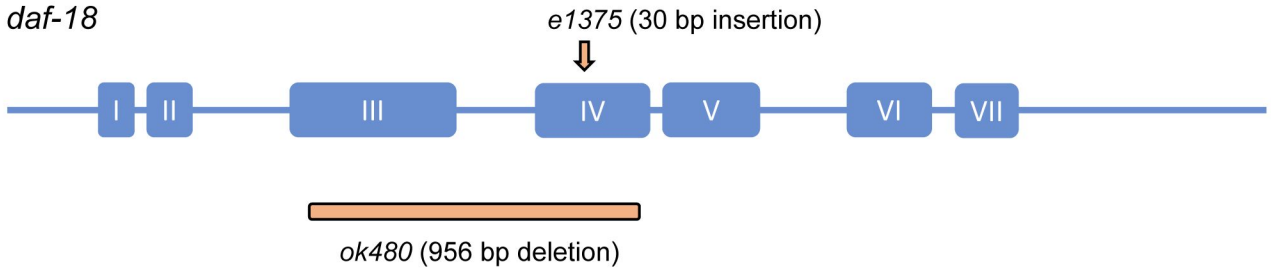

B.

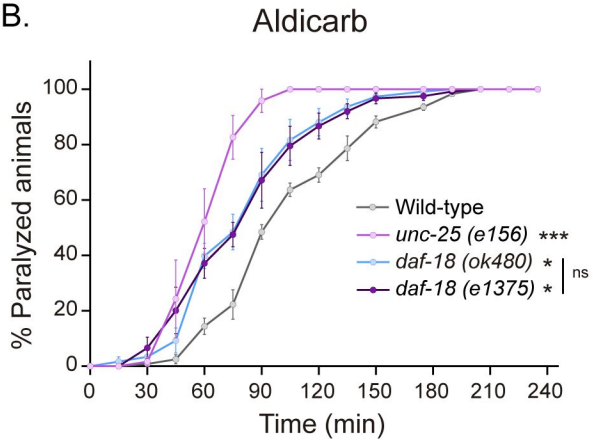

C.

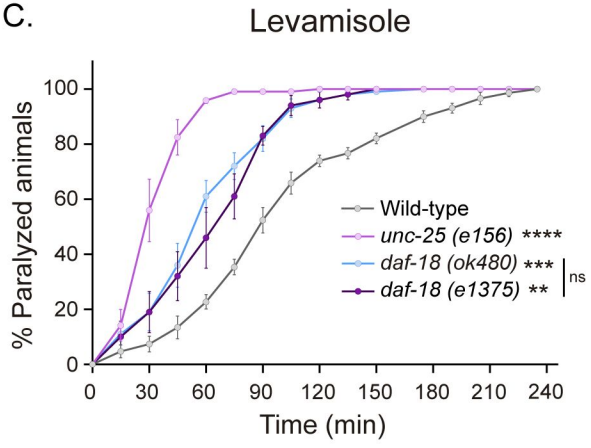

Suppl. Figure 2

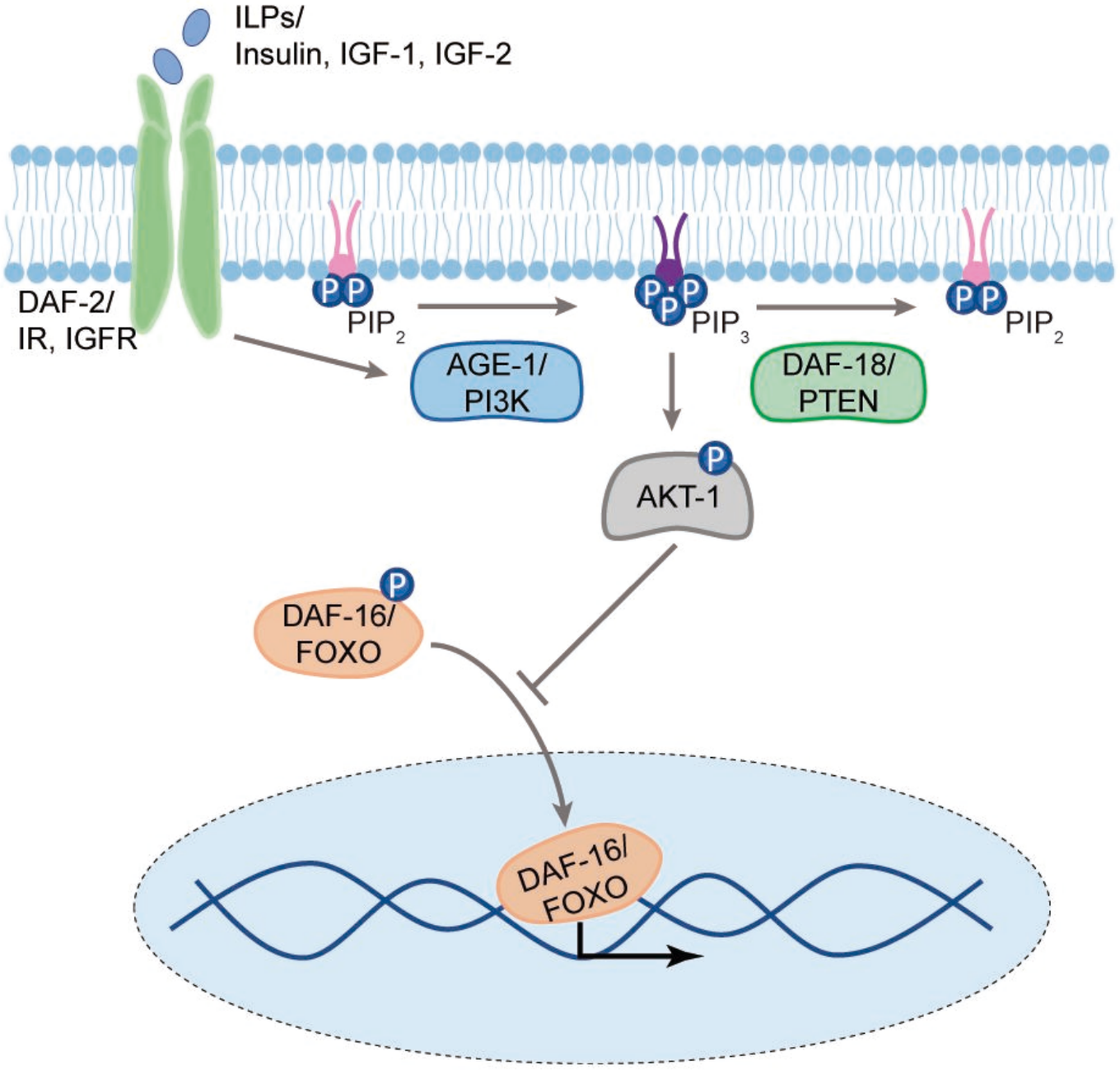

Suppl. Figure 3

A.

Punc-47::mCherry (GABAergic neurons)

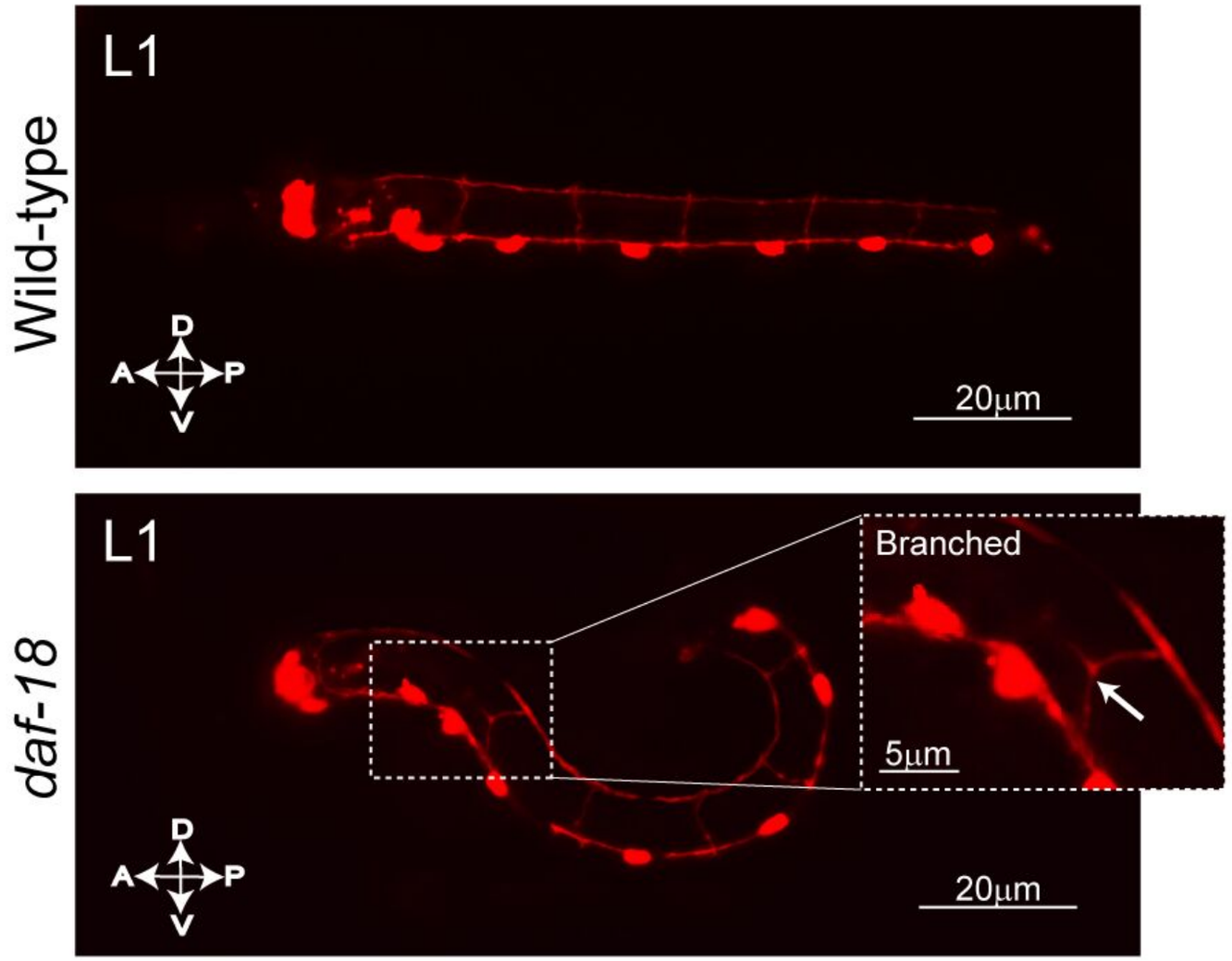

B.

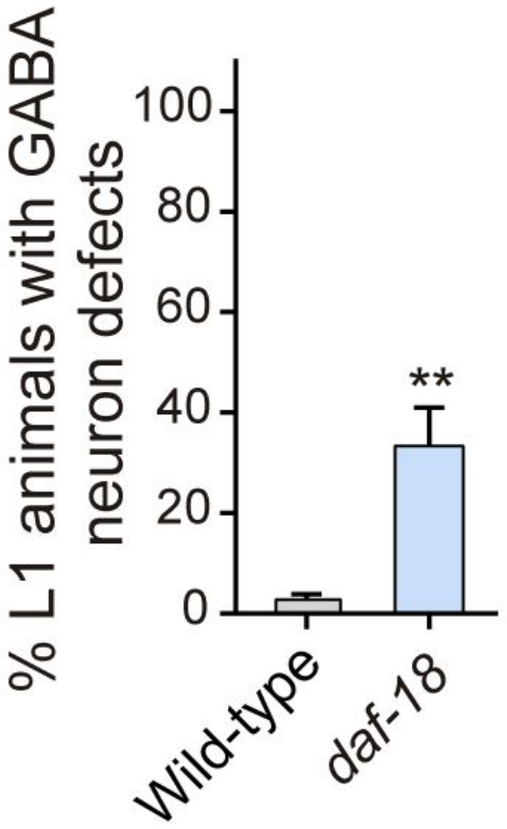

Suppl. Figure 4

A.

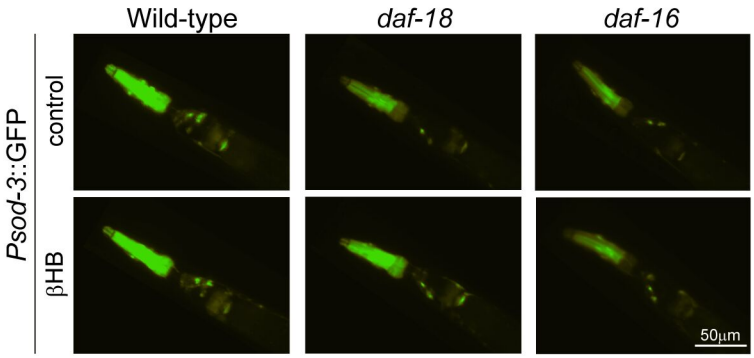

B.

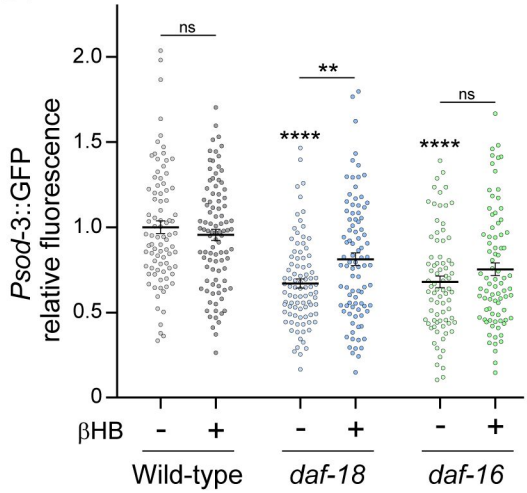

Suppl. Figure 5

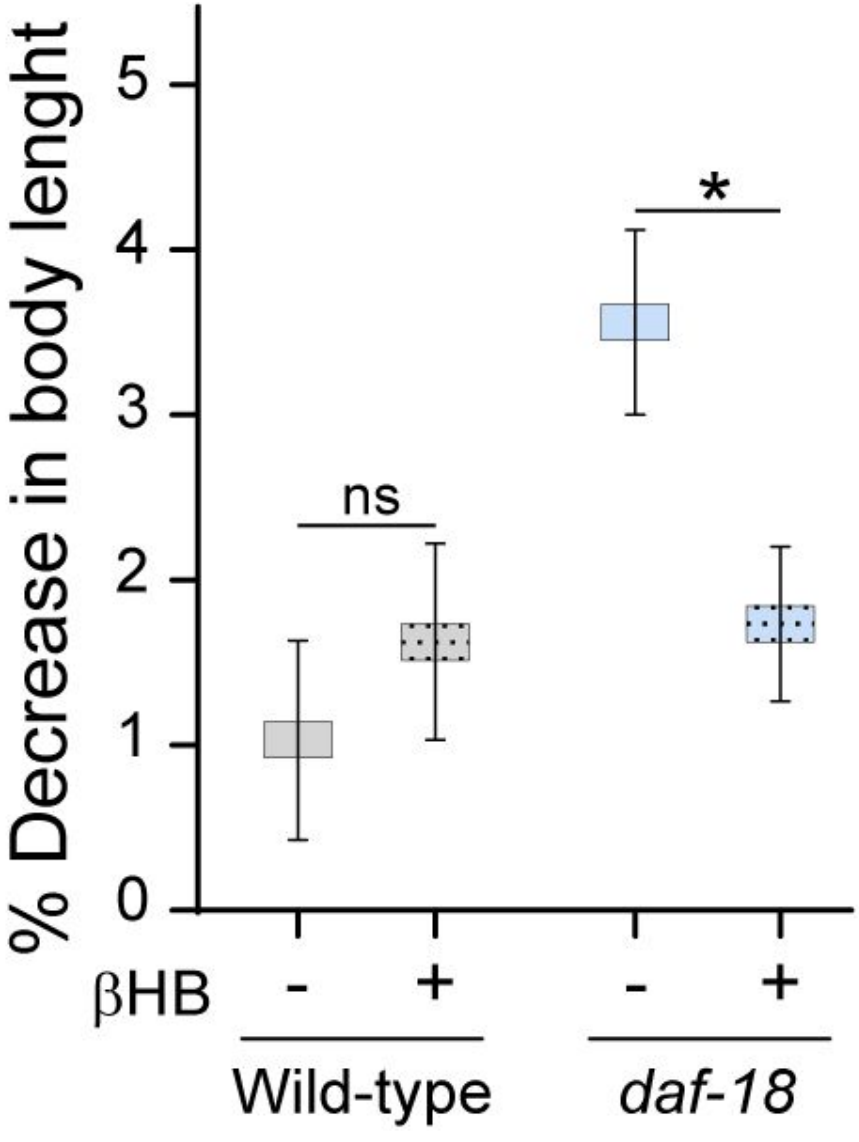

Suppl. Figure 6

A.

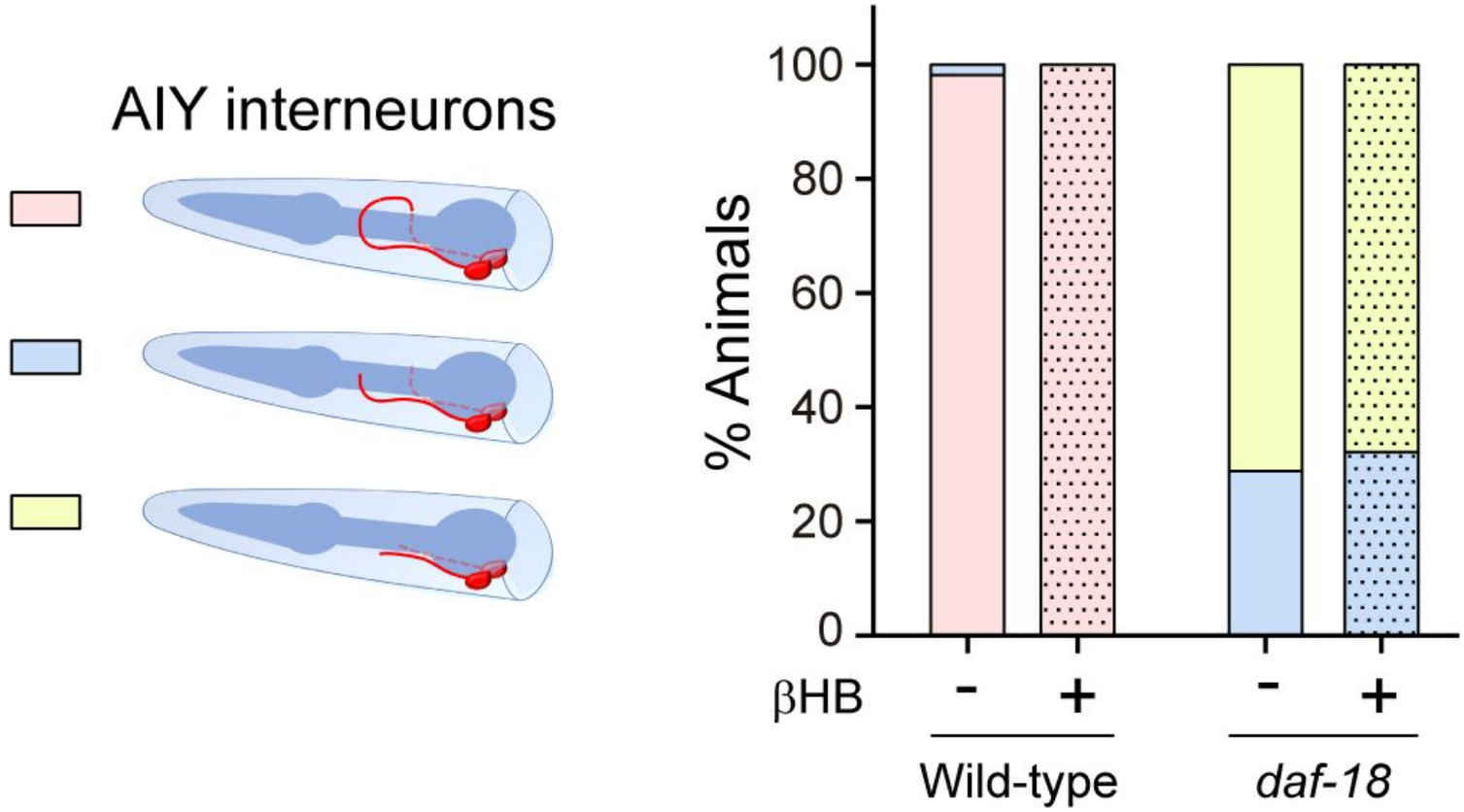
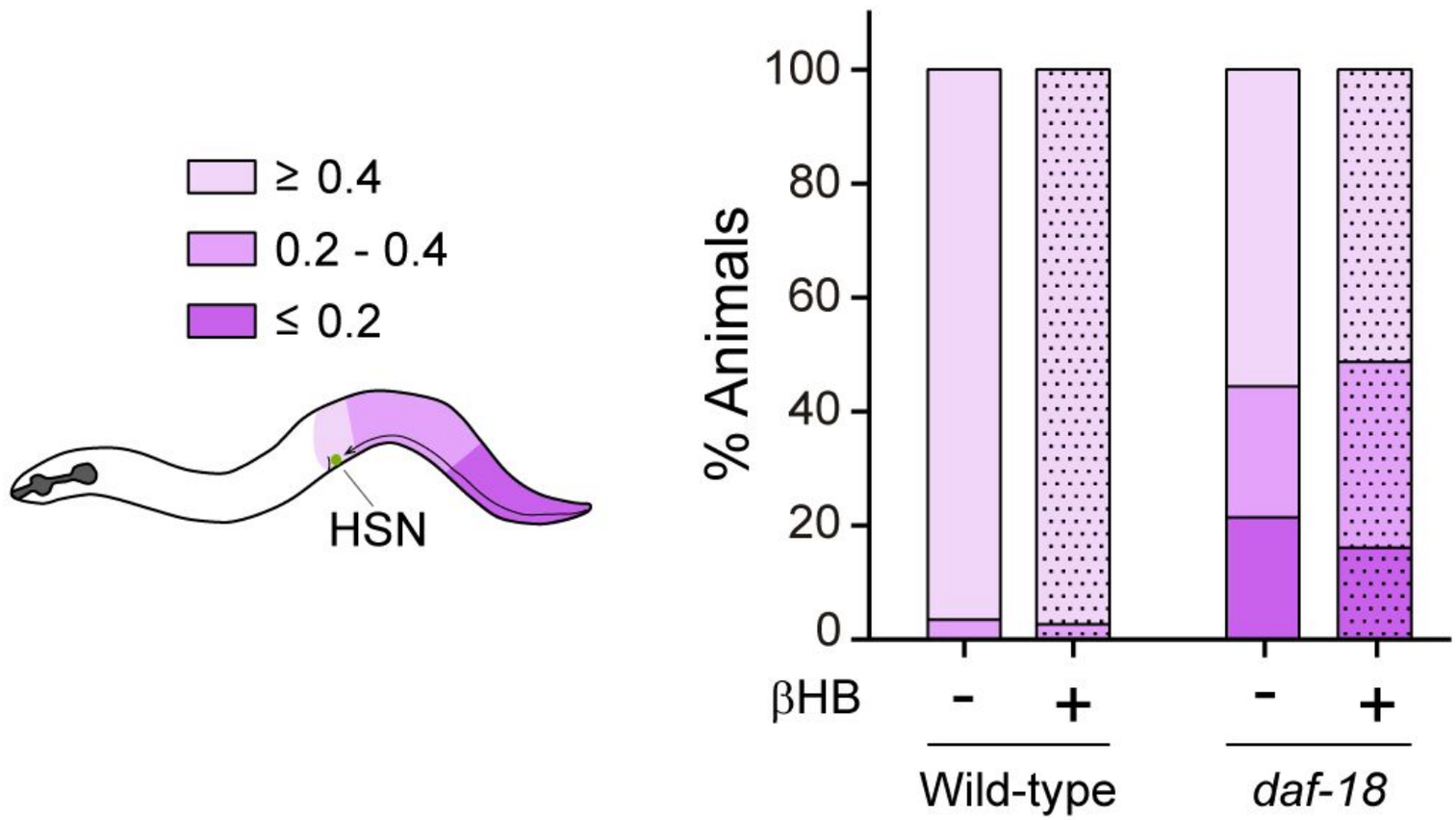
B.